Uncertainties in Target Definition for Radiotherapy of Peripheral Lung Tumours

Gitte Fredberg Persson

This review has been accepted as a thesis together with four previously published papers by University of Copenhagen May 10th 2011 and defended on June 10th 2011.

Tutors: Lena Specht, Stine Korreman, Per Munck af Rosenschöld and Anders Navrsted Pedersen

Official opponents: Dorte Nielsen, Matthias Guckenberger and Jan-Jakob Sonke

Correspondence: Department of Radiation Oncology, Rigshospitalet, Blegdamsvej 9, 2100 Copenhagen, Denmark

E-mail: gitte.persson@rh.regionh.dk

Dan Med Bull 2011;58(8):B4314

ORIGINAL CONTRIBUTIONS

The research was carried out from 2007 to 2010. The studies are described in an order relevant for the thesis not in the order of publication.

I. Persson GF, Nygaard DE, Hollensen C, Munck af Rosenschöld P, Mouritsen LS, Due AK, Berthelsen, AK, Nyman J, Markova E, Roed AP, Roed H, Korreman S and Specht L. Inter-Observer Delineation Variation in Stereotactic Body Radiotherapy of Peripheral Lung Tumours. Submitted.

II. Persson GF, Nygaard DE, Brink C, Jahn JW, Munck af Rosenschöld P, Specht L and Korreman S. Deviations in delineated GTV caused by artefacts in 4DCT. Radiother Oncol 2010, 96 (1), 61-66

III. Fredberg Persson G, Nygaard DE, Munck af Rosenschöld P, Vogelius IR, Josipovic M, Specht L and Korreman S. Artifacts in Conventional Computed Tomography (CT) and Free Breathing Four-Dimensional CT Induce Uncertainty in Gross Tumor Volume Determination. Int J Radiat Oncol Biol Phys. 2010 Dec 14. [Epub ahead of print]

IV. Persson GF, Nygaard DE, Olsen M, Juhler-Nøttrup T, Pedersen AN, Specht L and Korreman S. Can audio coached 4D CT emulate free breathing during the treatment course? Acta Oncol 2008, 47(7), 1397-1405

SUMMARY

Uncertainties concerning target definition in radiotherapy planning represent a serious challenge as they lead to systematic errors impacting the entire radiotherapy course. Breathing related artefacts in the planning computed tomography scan (CT) as well as uncertainties in the delineation of the gross tumour volume (GTV) can introduce systematic errors. In breathing correlated CT (4DCT) images of the patient throughout the breathing cycle are reconstructed based on a breathing signal. 4DCT has the ability to minimize breathing related artefacts compared to conventional CT but irregular breathing can cause inappropriate reconstruction and artefact. Respiratory audio coaching is a method to guide the patient to a more regular breathing and can be used during the acquisition of 4DCT.

This thesis consists of three studies investigating the extent and magnitude of uncertainties in volume definition for radiotherapy of peripheral lung tumours and one study exploring respiratory coaching. The first study (I) examined the inter-observer delineation variation for peripheral lung tumours treated with stereotactic body radiotherapy (SBRT). The inter-observer delineation variation was very small, although significantly larger in the CC direction compared to the transversal plane stressing that anisotropic margins should be applied. The second study (II) examined the impact of artefacts on delineated GTV size in 4DCT scans. For 16 out of 19 4DCT scans the GTV size variation throughout the bins was larger than could be explained by variation in delineation indicating the presence of artefacts. In the third study (III) conventional CT (3DCT), 4DCT and breathhold CT (BHCT) were acquired for 36 consecutive patients with 46 peripheral lung tumours. The GTV was delineated in all scans and compared with BHCT GTV size as a reference. The CT method significantly impacted the GTV size on average leading to an increase in GTV size in 3DCT and 4DCT when compared to BHCT indicating the presence of artefacts. The variation in GTV size was correlated to both tumour motion and breathing irregularity. The acquisition a BHCT as reference for tumour volume is recommended for lung tumour radiotherapy. The fourth study (IV) explored if respiratory audio coaching could improve the regularity of the breathing without changing the amplitude in a group of 13 volunteers. Respiratory audio coaching improved breathing regularity for the majority of volunteers, but introduced a significant although small change in breathing signal amplitude between free and coached breathing.

INTRODUCTION

Definitive radiotherapy can be compared to cancer surgery because both are local treatments aiming to eradicate malignant tumours. The surgeon can directly visualise the tumour and make sure that all macroscopic tumour with a suitable margin into the surrounding normal tissue is resected. Radiotherapy relies on radiological imaging of the tumour to direct the irradiation. Modern conformal radiotherapy planning based upon computed tomography (CT) scans with the addition of other imaging modalities e.g. PET for metabolic information and/or MR for better soft tissue resolution. For target definition and dose prescription the

radiation oncologist uses software tools to delineate the tumour (gross tumour volume, GTV) and adjacent high risk tissue. Due to the radiation sensitivity of vital tissues the therapeutic window in radiotherapy is narrow and a precise definition of the tumour and the surrounding normal tissue is therefore of the utmost importance.

Errors and margins in radiotherapy

Errors and uncertainties are inevitable in radiotherapy. Errors can be defined as the difference between a planned value and the actual value during treatment, however small they are [1]. Errors in radiotherapy occur both during the planning process and during the treatment delivery process and can be divided into systematic and random errors. Systematic errors in radiotherapy originate from imaging, image fusion when using multiple modalities and target delineation, but can also be introduced during patient setup and treatment delivery with organ motion, e.g. baseline shift of lung tumours or weight loss [2-4]. Systematic errors displace the delivered dose and can result in geographic miss of part of the tumour. Random errors are associated with patient positioning, but also with organ motion, e.g. due to breathing and heart beat. Random errors tend to even out over many fractions and translate into a blurring of the delivered dose. In a short course of radiotherapy, such as stereotactic body radiotherapy (SBRT), random errors simulate systematic errors and will have a greater impact on the delivered dose because of the fewer fractions and thereby lack of averaging effect [5,6].

To assure that the tumour is receiving the prescribed dose safety margins are added to the GTV as described in the ICRU (International Commission on Radiation Units & Measurements) Reports 50, 62 and 83 [7-9]. First a clinical target volume (CTV) is created by adding a margin to the GTV to account for the extension of microscopic disease. The actual microscopic disease extension is unknown in the individual patient and the magnitude of the CTV margin is often based on tradition and clinical experience since correlation studies between imaging and pathology are few and suffer from methodological challenges e.g. tissue shrinkage and deformation of tissue in the process of surgery and preparation for histological examination [10-12]. To ensure sufficient dose coverage of the CTV all uncertainties have to be considered and a planning target volume (PTV) is created by the addition of further margin [13]. According to the ICRU Report 62 [9] the motion of the tumour should be accounted for by creating an internal target volume (ITV). In the clinical setting it can be done in two different ways: By adding a separate ITV margin or by incorporating the tumour motion as an uncertainty into the planning target volume (PTV) margin. It has been suggested that the appropriate size of the PTV margin can be calculated in a probabilistic approach by considering all systematic uncertainties, all random uncertainties and also the width of treatment beam penumbra [14-16]. The beam penumbra can be described as the steepness of the dose fall-off from the field edge; the width of the penumbra primarily depends on the density of the tissue but also on parameters such as the shape of the multi-leaf collimator leaves [17]. The margin formula by van Herk et al. [15] is given in equation 1 and reflects that the systematic errors have a much larger impact than the random errors on the size of the PTV margin:

$$\text{PTV margin} = 2.5\,\Sigma + \beta\sqrt{\sigma^2 + \sigma_p^2} - \beta\sigma_p \qquad \text{(equation 1)}$$

Σ is the standard deviation of all systematic errors and σ is the standard deviation of all random errors. σp describes the penumbra and β is a parameter related to the prescribed minimum PTV dose level (β < 1 in SBRT). In low density tissue e.g. lung tissue, the beam penumbra is broad and the needed PTV margin for targets imbedded in lung tissue is smaller than for targets surrounded by solid tissue given identical random and systematic errors. Equation 1 is based on assumptions regarding tumour size and shape (should be large and round), number of fractions (should be large) and position variations (should be Gaussian distributed). These assumptions are not necessarily met in SBRT where tumours are small and the treatment is delivered in a few fractions.

Computed tomography and artefacts

A CT scan is a rotational x-ray imaging modality providing three-dimensional information on the internal anatomy of a patient. The x-ray tube and the detectors are mounted on opposite sides of a rotating gantry, measuring the attenuation of the x-ray beam through the patient while the couch with the patient is moving through the gantry. Multi-slice CT scanners are equipped with multiple rows of detectors in the longitudinal axis acquiring several image slices per rotation.

CT scans can be acquired in axial mode where one gantry rotation is performed before the table is moved to the next position or in helical mode where the table is moved continuously while the CT gantry is rotating and acquiring data. The pitch describes the propagation of the table per gantry rotation. With a helical scan further processing is needed to reconstruct the acquired raw data into axial slices. Depending on the scanner a 180 degrees or a full 360 degrees rotation of the CT gantry is typically necessary to reconstruct an image slice. The typical rotation time for a modern CT scanner gantry is between 0.5 and 1 second [18].

In order to perform consistent volumetric images from one-dimensional raw data acquired from multiple angles, the reconstruction algorithm is dependent on static conditions of the imaged object during CT acquisition. Volumetric images of the patient are created by digital mathematical processing, such as filtered back projection, transforming them into a grid [18]. The raw data consists of the measured detector signals during a scan and the angle in which they were acquired. From the grid a matrix consisting of picture elements (pixels) can be constructed. The number of pixels for a given matrix size determines the image resolution. However, the fundamental resolution is determined by the detector size. A voxel is a volumetric element corresponding to a pixel with a given slice thickness. The attenuation data of the voxels are transformed into a grey scale and quantitatively expressed as Hounsfield Units (HU) where 0 HU corresponds to the attenuation properties of water and -1000 HU corresponds to the attenuation properties of air [18]. Different reconstruction algorithms can be applied using different windowing on the HU scale, thereby enhancing different tissue types, e.g. bone, lung or soft tissue. The CT slices are then combined to construct full 3D volumetric images. Interpolations between slices are applied to reconstruct images in sagital and coronal planes. The image resolution of the 3D scan is anisotropic as the resolution in the transversal plane is typically better than in the longitudinal plane. To increase the image resolution in the longitudinal plane, thinner slices can be used with the detector size being the lower limit.

During the acquisition of a CT scan, motion within the scanned volume can result in image artefacts. Motion with a time span shorter than seconds can affect the single CT slice, and motion within seconds to minutes can affect the reconstructed image of tumours and organs. Breathing related lung tumour

motion is well known as a cause of volumetric deformation of the tumour image [19-21]. The degree of deformation of the images is impacted by several factors: the rotation time of the CT gantry, the extent and velocity of tumour motion, slice thickness and number of detector rows [18,19,21]. An additional source of artefacts is the reconstruction of a spiral scan into planar images [18]. Examples of different artefacts are given in figure 1. Blurring in the periphery of the tumour can represent both "partial volume effect" and "partial projection effect for moving objects" both occurring within a single CT gantry rotation. The partial volume effect is caused by the averaging of the attenuation properties of the tissue within the voxels of the CT scan and is especially present in the interfaces between tissues with large differences between densities such as tumour and lung. The partial projection effect for moving objects is caused by motion faster than the CT gantry rotation, e.g. a tumour moving due to respiration or the heart beat [21-23]. Other artefacts such as duplicate, incomplete or overlapping structures occur at the interface between adjacent CT gantry rotations and are also caused by organ motion [23].

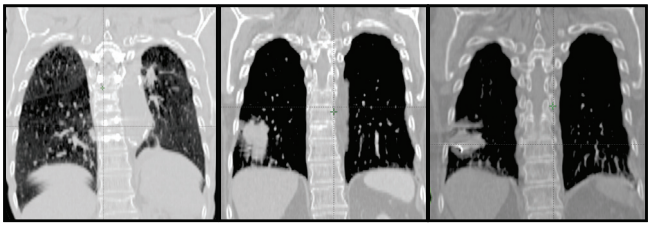

Figure 1
Examples of breathing induced image artefacts in coronal 3DCT images: Overlapping contours and smearing of the right diaphragmatic dome (left). Overlapping structures and smearing of the caudal part of the tumour in the right lung (middle). Duplicate structures are seen in the tumour in the right lung (right).

Breathing correlated computed tomography (4DCT)

A basic assumption in radiotherapy is that the planning situation must simulate the treatment situation as precisely as possible. Therefore, imaging for radiotherapy planning is routinely performed with the patient breathing freely or shallowly (as opposed to diagnostic imaging performed with voluntary breathhold). This constitutes a major challenge in the treatment of thoracic tumours as conventional CT scans (3DCT) are prone to breathing related artefacts. For the majority of lung tumours, breathing related motion is modest, e.g. only 10 % of tumours have a peak-to-to peak motion exceeding 1 cm [24]. However, the motion varies with the tumour location, and peak-to-peak motion of more than 3 cm during free breathing is seen for tumours located near the diaphragm [4,25].

In 3DCT it is well known that such tumour motion can cause volumetric deformation of the tumour image [19]. Four-dimensional computed tomography (4DCT) is a tool for the evaluation of tumour motion and the minimization of breathing related artefacts compared to 3DCT. It provides a predefined number of time-resolved reconstructed CT scans (bins) of the patient throughout the breathing cycle [23,26-32]: A CT scan with a very low pitch and oversampling of images is acquired simultaneously with the recording of a breathing signal.

The breathing signal can originate from the motion of an external marker, flow or temperature of the breath or an internal marker such as the moving diaphragm or the changing lung volume [30,32,33]. The individual time stamped CT images are sorted into bins based on the co-registered breathing signal.

The reconstruction of a 4DCT scan is exemplified in figure 2. In the example the CT slices are divided into 6 bins although 10 bins are more commonly used. A 4DCT scan provides a time resolved image of the tumour and has the potential to decrease the presence of artefacts compared to 3DCT. Nevertheless, irregular breathing and large tumour motion may still cause artefacts in the 4DCT scan because of improper binning and residual motion within the bins (intra phase motion).

The images of a 4DCT scan can be binned either according to amplitude or phase of the breathing signal, or to a combination of these [21,30,32,34-36]. Amplitude-binning relies on a strong correlation between the amplitude of the breathing signal and the tumour position, in which case it can provide small residual motion within the bins [35] compared to phase binning. A disadvantage can be a relative undersampling of images in some bins leading to artefacts in cases of large motion within a short time [34]. Phase-binning ensures bins equally spaced in time. However, artefacts can arise from large residual motion within some of the bins as well as irregular breathing causing mismatch in reconstruction of the respiratory phases. Phase-shifts between tumour motion and the expiratory breathing signal during CT acquisition will result in artefacts irrespective of the binning method [21,23,27].

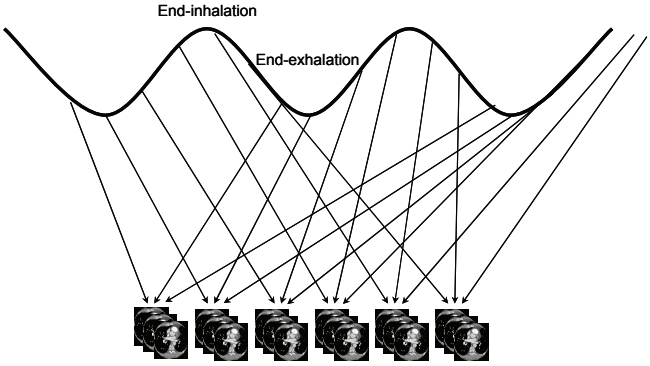

Figure 2
Schematic illustration of a 4DCT reconstruction process with six bins created based on respiratory phases of the breathing signal

Uncertainty in delineation

Target delineation is overall a major source of uncertainty and contributes heavily to the systematic errors in radiotherapy. The true GTV in the individual patient is unknown; hence the delineation uncertainty can only be estimated. An often used approach is to examine the delineation variation in a group of observers delineating the same target [37-41]. The delineation variation will depend on the tumour, the surrounding tissue, the imaging modality, the observers, and the delineation protocol. Steenbakkers et al. [38] evaluated the delineation variation for tumours, in patients with locally advanced lung cancer, with CT +/- 2-□18F□-fluoro-2-deoxy-D-glucose (^{18}F-FDG) positron emission tomography (PET) and they found that the addition of PET dramatically decreased the delineation variation. Furthermore, the delineation variation was much larger in areas where the tumour adjoined the mediastinum or in presence of atelectasis, than where the tumour adjoined the lung or the chest wall. The integration of PET/CT adding metabolic information to radiotherapy planning has had a major impact, altering radiotherapy planning in two ways: 1) guidance to detect additional metastatic lymph nodes or distant metastasis and thereby influencing the staging of the

disease; and 2) guidance to distinguish between tumour and surrounding tissue with similar density, e.g. the mediastinum or atelectasis, in the GTV delineation process [38,42-46]. For peripheral lung tumours surrounded by lung tissue or visceral pleura the impact of PET information on GTV delineation is however shown to be limited [47].

Current recommendations include a multidisciplinary approach, with input from both radiologists, nuclear medicine physicians and oncologists, in the target definition process in order to decrease variability [48,49].

Respiratory coaching

An approach to minimize breathing related artefacts in imaging for radiotherapy planning is to apply breathing guidance, i.e. respiratory coaching or guided breathhold. In a breathhold CT scan (BHCT) neither breathing motion nor irregular breathing will impact the tumour image. However, a positional error will be introduced unless the patient can be guided to reproduce the depth of the breathhold during treatment. Respiratory coaching has the potential to guide the patient to a uniform breathing pace and depth during the acquisition of a planning scan thereby minimizing the risk of artefacts in the scan. Respiratory audio coaching can be applied by audio-prompting, where a voice or sound lets the patient know when to breathe in and out. It facilitates a more regular breathing pace but tends to induce a deeper breath (larger amplitude of the breathing) [50,51]. For visual coaching a screen or a pair of goggles are needed, and the patient is visually guided by moving bars or curves to inhale or exhale. Visual coaching facilitates a regular breathing depth [50,51]. Respiratory coaching thus changes the breathing and tumour motion, and a 4DCT acquired with respiratory coaching may not be representative of the tumour motion during the patient's free breathing.

Breathing adapted radiotherapy

There are several approaches for applying breathing adaptation in radiotherapy of lung tumours with different degrees of complexity [52]. Most simple is to apply breathing adaptation primarily in the treatment planning process by using 4DCT thereby avoiding the positional error potentially introduced by using a conventional free breathing CT capturing the tumour in an arbitrary position. Generally, there are three different ways to use the 4DCT for planning. The use of a midventilation bin (MidV) best representing the tumour's time weighted midposition for treatment planning and incorporation of the tumour motion amplitude (intra-fraction motion) into the PTV margin [53]. A motion encompassing volume for planning can be created by delineating a composite GTV of all or some bins or by delineating the GTV in a "maximum intensity projection" (MIP) scan based on the 4DCT data set to create an individual ITV margin [52,54,55]. When comparing the MidV and the ITV approach, the MidV approach results in smaller treatment fields [56], but no comparative clinical trials have been performed. The third option is using a bin representing a pre-specified breathing phase with the purpose of treatment with respiratory beam gating in this phase [57,58]. In case of breathhold gating, the 4DCT is replaced by a 3DCT acquired during controlled breathhold [59,60]. In all cases of using 4DCT artefacts may impact the size and shape of the delineated GTV, although probably to a lesser extent with the motion encompassing volume (where the artefacts are superimposed by tumour projections from other bins). Radiotherapy planning on a bin representing the midventilation phase (MidV) is most likely to be impacted by breathing related artefacts because residual tumour motion and velocity are often large in this breathing phase [21].

Much effort has been done to develop breathing adapted treatment strategies to compensate for breathing related tumour motion. Set-up to the tumour's midposition either by applying breathing correlated image guidance as daily 4D conebeam CT (CBCT) [5,61-64] or a slow 3D CBCT [65-67] is for most patients the most effective method to decrease the systematic errors introduced by tumour motion and thereby decrease the magnitude of the needed PTV margin [5,68-70]. Other more advanced options for breathing adapted treatment are available: Respiratory gating where the linear accelerator is prompted only to deliver radiation in a pre-specified part of the breathing cycle [57,58]. The advantages of this method are that tumour motion during beam-on can be minimised (especially when gating in the stable expiration phase) and that the anatomical changes happening during breathing can be translated into sparing of normal tissue (with inflation of the lung in deep inspiration gating) [52,71]. A limitation to the gating technique is the longer treatment time as treatments are only given in a fraction of the breathing cycle (duty cycle). New treatment strategies combining the MidV approach with gating offers longer duty cycles with a decrease in margins [72]. This approach could be promising for tumours with large motion. The most technically advanced solution is tumour tracking were the treatment beam follows the motion of the tumour during the breathing cycle. This option is still not fully clinical available except in cases of very small tumours using the CyperKnife (Accuray Inc., Sunnyvale, CA, US) [73,74]. Different approaches, e.g. DMLC (dynamic multi-leaf collimator) or robotic couch tracking are being developed [75-79]. Both respiratory gating and tumour tracking depend on a stable correlation between a surrogate for breathing and tumour position. Both methods are sensitive to phase and baseline shifts, especially when external markers are used to monitor the breathing.

Stereotactic body radiotherapy (SBRT)

SBRT refers to a high precision hypo-fractionated treatment of tumours outside the brain [80]. It is widely used in the treatment of peripheral lung tumours, e.g. medically inoperable early stage lung cancers and solitary or oligo-metastases in the lung [80]. Classical SBRT was applied with the patient immobilised within an external frame with an extra coordinate system used for setup [81]. Today most centres use a frameless approach with the patients immobilised in a supportive system combined with extensive use of in-room imaging [5]. The treatment planning technique was adopted from the cranial stereotactic treatments with its use of extreme hypo-fractionation, multiple-angled beams and steep dose gradients. By tradition PTV margins have been very tight and in many centres no CTV margin has been added, i.e. the GTV and CTV are considered identical [80]. Nevertheless, prospective phase II trials report local control rates for early stage non small cell lung cancer (NSCLC) after SBRT in the range of 40 % to 98 % [82-86] depending on tumour size and radiation dose [87-89].

AIM AND HYPOTHESES

The overall aim of this thesis was to investigate uncertainties impacting target definition in radiotherapy of peripheral lung tumours. The thesis was based on the following hypotheses:

- The magnitude of inter-observer delineation uncertainties for peripheral lung tumours in patients referred for SBRT can

be estimated and will be low due to the high gradient in density between tumour and lung tissue. However, the inter-observer delineation uncertainty in the cranio-caudal direction will be larger than in the transversal plane due to the anisotropic image resolution in computed tomography. Study I investigated the inter-observer delineation variation for peripheral lung tumours in patients referred for SBRT.

- Artefacts in 4DCT scans will impact the size of the delineated GTV for peripheral lung tumours and the volumetric impact will be correlated to the magnitude of tumour motion as well as to the irregularity of the breathing. In study II and III, deviations of GTV size in 4DCT scans of patients with peripheral lung tumours were analyzed. Deviations in GTV size were correlated to tumour motion and breathing regularity.
- With the purpose of optimizing the image quality in 4DCT, it will be possible, by using a person's natural breathing frequency for respiratory audio coaching, to obtain a more stable breathing without changing the breathing cycle amplitude? Study (IV) investigated the impact of respiratory audio coaching on the variation in breathing cycle amplitude.

METHODS

This section gives an overview of the methods used in the four studies. A more detailed explanation is given in the separate manuscripts in the appendix section.

Patients and volunteers

The primary focus of the thesis is on artefacts in CT scans and delineation uncertainties in the planning of lung tumour radiotherapy. In two of the studies variation in delineated GTV size is used to measure the impact of artefacts, which makes the distinction between volume variation caused by delineation uncertainty and artefacts crucial. Lung tumours embedded in lung tissue have a steep tissue density gradient, making tumour definition much easier than for tumours in the hilar region or mediastinum, where the tissue density gradient is less steep. By studying peripheral lung tumours the contribution from delineation uncertainty is minimized. Exclusion criteria in the studies were tumours extending into the thoracic wall or large vessels and tumours inseparable from fibrosis or atelectasis, as these features increase delineation uncertainty.

Three different groups of patients and a group of volunteers were included in the four studies:

- Patients with early stage NSCLC ($T_{1\text{-}2}N_0M_0$) referred for stereotactic radiotherapy at Rigshospitalet, Copenhagen University Hospital and Odense University Hospital.
- Patients with oligo-metastases to the lung (1-4) referred for stereotactic radiotherapy at Rigshospitalet, Copenhagen University Hospital.
- Patients with locally advanced NSCLC ($T_{1\text{-}2}N_{1\text{-}3}M_0$) referred for fractionated radiotherapy with curative intent at Rigshospitalet, Copenhagen University Hospital.
- Volunteers - mainly nurses - recruited among the staff in the Department of Radiation Oncology at Rigshospitalet, Copenhagen University Hospital.

Different selection criteria were used for the different studies and no patients were included in more than one study.

In the inter-observer delineation uncertainty study (I) all patients treated with stereotactic radiotherapy at Rigshospitalet in 2008 were eligible. Four patients were excluded from analysis because of missing CT scans leaving 22 patients with 26 tumours for inclusion in the study. The majority of patients had early stage NSCLC and only three of the patients had a solitary lung metastasis.

The second study (II) included two selected groups of patients; eight patients with early stage NSCLC planned for stereotactic radiotherapy at Odense University Hospital (Group A) and eleven patients with locally advanced NSCLC planned for fractionated radiotherapy with curative intent at Rigshospitalet (Group B). Group A had amplitude binned 4DCT scans and were not selected based on tumour motion. Group B had phase-binned 4DCT scans and tumours moving 0.5 centimetres or more in the cranio-caudal direction. Inclusion criteria for both groups of patients were peripheral lung tumours free of the mediastinum and with no atelectasis. Only peripheral tumours were included in the analysis.

The third study (III) included a cohort of patients planned for stereotactic radiotherapy at Rigshospitalet in the time period from February to December 2009. Forty-three consecutive patients were eligible of which seven patients were excluded for the following reasons: tumour extending into the thoracic wall (1), tumour extending into the descending aorta (1), tumour inseparable from fibrosis or atelectasis (3) and one patient for whom a PET/CT was not acquired. A total of 36 patients with 46 tumours were included.

The last study (IV) was a pilot study exploring the impact of respiratory coaching on the breathing amplitude and included 13 volunteers. The volunteers were mainly staff from the Department of Radiation Oncology, RH. One of the originally included volunteers was excluded as this volunteer was not able to follow the coaching instructions, leaving 12 volunteers for the analysis.

Acquisition of 3DCT scans (I, III)

The PET/CT scans used to analyze inter-observer delineation variation in study I and to analyze artefacts in 3DCT in study III were performed on a Siemens Biograph^{TM} scanner (Siemens AG, Munich, Germany). The scanner has 24 detectors but only the central 16 are used for the PET/CT scan. Each detector measures 0.75 mm in total giving a collimation of 12 mm. CT scans were performed in a helical mode with a pitch of 1.2. The scans were reconstructed with a slice thickness of 3 mm. One patient in study I only had a conventional CT performed (no PET) and in this case the CT scanner was a Siemens Sensation Open^{TM} (Siemens AG, Munich, Germany) scanner with a collimation of 24 detectors each measuring 1.2 mm. A helical scan mode with a pitch of 1.2 was used. The scan was reconstructed with a slice thickness of 2.5 mm. The rotation time was 1 s for both scanners. The patients were immobilized with arms above their head using a VacFix® vacuum cushion in a Styrofoam shell and were scanned during free breathing. Intravenous contrast enhancement was used for all patients.

Acquisition of 4DCT scans (II, III)

In study II both amplitude and phase-binned 4DCT scans were analyzed. Eight patients (group A) from Odense University Hospital were included. The patients were immobilised in a stereotactic body frame using a VacFix vacuum cushion and were scanned during free breathing. A Siemens Somatom 4 multi-slice scanner (Siemens AG, Munich, Germany) was used to acquire the 4DCT in cine mode. Ten detector rotations were completed for each table position and rotation time was 0.5 second. The scan was reconstructed with a slice thickness of 2.5 mm. The acquisition period was fixed for all patients regardless of the period of the breathing cycle of the individual patient. The respiration signal was based

on temperature changes of the patients' breath measured by a thermocouple in a facial mask [90] and consisted of relative temperature over time. In-house made software was used for amplitude binning of the CT slices. In case of undersampling within the bins, interpolations were performed to complete each of the ten bins. The amplitude-binned 4DCT scans were constructed post treatment and not used for actual treatment planning.

The eleven phase-binned 4DCT scans (group B) analyzed in Study II and all the 4DCT scans analyzed in study III were acquired at a Siemens Sensation Open multislice CT scanner in a helical scanning mode. The scanner has a collimation of 24 detectors each measuring 1.2 mm. A slice thickness of 3 mm with an increment of 2 mm was reconstructed. The pitch was 0.1 and there was a one second rotation time. The patients were immobilised in a VacFix vacuum bag and scanned during free breathing. The Real-time Position Management (RPM) 1.8 system (Varian Medical Systems, Palo Alto, CA, US) was used to track and record the respiratory signal. After the scanning procedure was finished, the automatically identified end-inspiration peaks were evaluated and if necessary manually corrected in the RPM software. The breathing signal was transferred to the Siemens scanner computer and the CT images were sorted into ten bins according to phase of the breathing signal, starting at end-inspiration. The ten bins were equally spaced in time over each breathing cycle.

Acquisition of breathhold CT scans (III)

The BHCT scans in study III were acquired immediately after the 4DCT in the same session and on the same scanner in a helical scan mode with a pitch of 1.2. The patients were asked to take a deep inspiration and hold it during the scan. The respiration signal was monitored using the RPM system during the scan. In case the breathhold was not stable a new BHCT scan was obtained. The scan was reconstructed with a slice thickness of 3 mm.

GTV delineation (I-III)

GTV delineations were all performed using Eclipse software (Varian Medical Systems, Palo Alto, CA, USA). A broad window setting was used (-1000 to 700 Hounsfield Units) allowing for visualisation of both lung tissue and structures in the thoracic wall. In study II and III all delineations were performed by the same observer and for each patient all GTV delineations in all scans were performed within the same session to minimize the intra-observer variation. GTV size was measured using a dedicated software function in eclipse.

Analysis of inter-observer delineation uncertainty (I)

The cohort of 22 patients treated with stereotactic radiotherapy all had a PET/CT scan performed for treatment planning. As a part of the clinical routine the PET/CT was first analyzed by a specialist in nuclear medicine together with a radiologist as the first step in the planning procedure. The PET/CT scan was performed as a whole body scan and was systematically analyzed to assure that the disease had not metastasized or developed further in which case the treatment might be changed. The PET positive lesions were then roughly marked by the specialist in nuclear medicine. The PET contour was not a reference contour and was only used as a pointer to where the lesion was. Our delineation protocol prescribed that the contouring was done on the CT scan and not the PET. Only in cases of atelectasis or if the tumour was difficult to distinguish from mediastinal structures was the rough PET contour used to delineate the GTV. This is rarely the case with peripheral lung tumours.

For the study, the 22 CT scans with PET contours, but without the primary contours used for the clinical plan, were exported to a separate Eclipse (Varian medical systems) research database.

Six observers; three radiation oncologists and three radiologists independently delineated the GTV for each for the 26 tumours. Delineations of GTVs were performed independently by the six observers, with a fixed broad lung window (-1000 to 700 HU). The magnification factor was left to the observer to decide and the rough PET contour could be switched off during the delineation. The observers were asked to delineate the GTV without changing the window setting and according to ICRU 50 guidelines "the gross visible extent and location of the malignant growth" [8] and thus not include any assumed uncertainties.

The data-file (dicom) of the six contours for each tumour was extracted from Eclipse and analyzed in MATLAB, version 2007b (The MathWorks Inc. Natick, MA, US) Three different types of analysis were made. Calculation of concordance indexes, calculation of volume differences and calculation of standard deviations (SD) of the delineation variation were made for each tumour, and means and SDs were calculated for the whole cohort of patients.

The concordance index (CI) was calculated as the mean of the ratios between the volume of intersection and the union volume calculated pair wise for all combinations (15 pairs) of GTVs of each tumour. The CI was also calculated for the group of oncologists and radiologists separately. The CI can vary between 0 and 1. A value of 1 will indicate complete agreement among the observers and a value of 0 would indicate complete disagreement among the observers.

To examine what was the impact of delineation uncertainty on delineated GTV size, the GTVs for all observers for all tumours were measured by a software tool in Eclipse. For each tumour the absolute and relative differences between the largest and the smallest delineated GTV size were calculated.

The SD of the delineation variation was calculated separately for the transversal plane and the CC direction respectively. This was done as it matches the way the delineations are performed on CT – slice by slice – and because the inter-observer delineation variation in the CC direction is more dependent on the slice thickness.

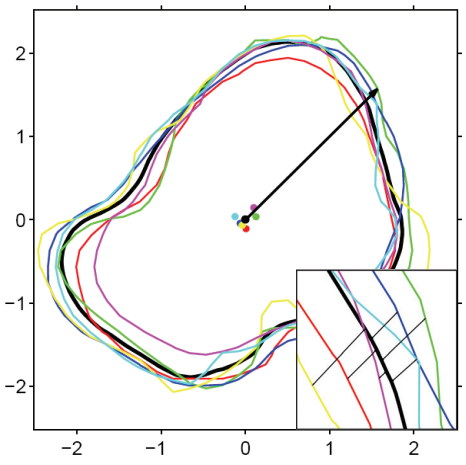

Figure 3

Schematic drawing of a CT slice with the contours of all six observers, each in a different colour (the magnitude of the x- and y-axis is cm). The coloured dots are the respective centre of volumes and the black dot is the mean position. The black contour is the mean contour computed as the mean distance from the reference point to the contours in 360 equally spaced angles. A local SD of the distances from the contours to the mean contour was calculated in the same 360 equally spaced angles as indicated by the inserted magnification.

For the transversal plane each slice was analyzed separately. A minimum of two contours had to be drawn for a slice to be included in the analysis of the observer variation in the transversal plane. For each slice the mean position of the centres of volume (CoVs) of all contours was found and used as a reference point. In figure 3 is shown a CT slice with six contours each in a different colour. The coloured dots are the respective CoVs and the black dot is the mean position. A mean contour was computed (black contour) as the mean distance from the reference point to the contours in 360 equally spaced angles deviating from the reference point. A local SD of the distances from the contours to the mean contour was calculated in the same 360 equally spaced angles as indicated by the inserted magnification in figure 3. The mean of all local SDs in all slices was considered the tumour specific delineation uncertainty in the transversal plane (SD_{trans}). The mean of the 26 tumour specific SD_{trans} was considered the population specific delineation uncertainty in the transversal plane.

For analysis of inter-observer delineation variation in the CC direction, a reference point was found as the mean of coordinates of the x-, y- and z-direction of the CoV of the six volumes. A caudal and cranial mean plane was calculated as a mean of the six distances from the reference point to the most caudal and cranial slice of each contour. The distances from the most caudal slice of each contour to the caudal mean plane (6 distances) and from the most cranial plane of each contour to the mean cranial plane (6 distances) was calculated and the SD of these 12 distances was considered a measure of the tumour specific inter-observer delineation variation in the CC direction (SD_{cc}).

The mean of all tumour specific SD_{cc} was considered the overall inter-observer delineation variation in the CC direction. The SD_{trans} and SD_{cc} were also calculated separately for the group of oncologists and radiologists respectively.

Tumour volume was calculated as the mean of the GTVs delineated by the six observers. Correlation analysis was computed between tumour size and SD_{trans} and SD_{cc} respectively.

Analysis of intra-session delineation variation (II)

To be able to differentiate between the impact of delineation uncertainties and artefacts, the intra-session delineation uncertainty was estimated. In eight 4DCT scans (group A, study II) the GTV was delineated twice in all bins within one session. The re-delineations were performed immediately after the primary delineations. During the re-delineation procedure the observer was blinded to the initially delineated GTV. The relative deviations between the size of the initial and the re-delineated GTV were calculated for each bin. All relative deviations from all bins and all eight patients were pooled and the SD calculated. As a reasonable measure of the magnitude of volume deviations caused by intra-session delineation uncertainty in study II, 2SDs of the pooled relative deviations between the two delineations was chosen and GTV size deviations exceeding this value were considered to be caused by artefacts.

Analysis of GTV size deviations (II, III)

In study II and III, deviations from a reference volume were used as surrogate measures for the impact of artefacts on the delineated GTV. As the true GTV size for the individual patient was unknown, GTV size in the end-expiration bin (GTV_{exp}) and GTV size from a breathhold scan was used as references for GTV size in study II and III respectively.

In study II GTV_{exp} was used as reference volume in the analysis, as the expiration phase is typically the most stable phase in the breathing cycle [16]. The deviation of GTV in all bins from the reference GTV_{exp} was calculated. To differentiate the impact of artefacts on GTV delineation from that of delineation uncertainty, the maximal value of the numeric deviations of GTV sizes throughout the 4DCT from GTV_{exp} (Dev_{max}) was calculated for each patient and compared to the magnitude of the volume deviations caused by intra-session delineation uncertainty.

In study III a voluntary inspiration breathhold scan of each patient was acquired and the GTV size from this scan (GTV_{BH}) was used as a reference volume. The GTV size in the 3DCT (GTV_{3D}), in the end-inspiration bin of the 4DCT (GTV_{insp}), the midventilation bin of the 4DCT (GTV_{MidV}) and the end-expiration bin of the 4DCT (GTV_{exp}) were compared to the reference GTV_{BH}. The Wilcoxon paired rank test was used for the comparisons. Both absolute and relative deviations were calculated. The relative numeric difference was also calculated as both negative and positive deviations from the reference GTV_{BH} were hypothesized to be equally caused by artefacts.

In both studies a coefficient of variation (CV_{GTV}) was calculated for each tumour as the standard deviation (SD) of the GTV sizes in all bins throughout the 4DCT divided by the mean GTV size of the 4DCT. The CV_{GTV} is used as a measure of volume variation independent of tumour size.

The end-expiration and end-inspiration bins were identified visually as the phases with the most caudal (inspiration) and cranial (expiration) position of the diaphragmatic dome ipsilateral to the tumour.

Tumour motion (II, III)

Tumour motion in left-right (LR), anterior-posterior (AP) and cranio-caudal (CC) directions was measured as the peak-to-peak displacement of the CoV of the delineated GTVs throughout the ten bins of the 4DCT. As large tumour motion can result in artefacts in both 3DCT and 4DCT, we tested for a correlation between tumour motion in the CC direction and surrogate measures of artefacts (CV_{GTV} and deviations from the reference volumes).

Identification of the midventilation bin (II, III)

The geometrical centre of the GTVs, within each 4DCT, was found as the mean of the CoVs of the ten GTVs. For the amplitude-binned 4DCT scan (group A, study II) the CoVs of the separate bins were weighed with a time-factor. The phase-binned 4DCT scans (group B, study II and study III) were already equally spaced in time due to the binning method. The bin with the GTV CoV closest to the geometrical centre of was considered the midventilation bin.

Respiratory coaching (IV)

In study IV respiratory data from repeated coaching sessions of twelve volunteers were analyzed. The first coaching session simulated the planning situation and was considered a reference session. The following two sessions were simulating treatment sessions. In this thesis only data from the reference session is described and analyzed. The coaching session began with a recording of 120 s free breathing. The breathing signal of the free breathing was analyzed and by visual evaluation the typical duration of the volunteers in- and expiration phases was measured. Two different coaching approaches were used: For the first coaching approach (coaching 1) the typical duration of the in- and expiration phases during free breathing were used to pace the

coaching. After the first coaching the volunteer could adjust the length of the in- and expiration intervals aiming at a comfortable and natural breathing and this adjusted pace was used for the second respiratory coaching (coaching 2). The pace of the audio coaching was mediated by a recorded female voice saying "in" and "out". After each coaching session the volunteers were asked which of the coaching approaches they preferred.

Analysis of respiratory data (II – IV)

In study II two different methods to acquire a respiratory signal were used. For the patients in group A the respiration signal was based on temperature changes of the patients' breath measured by a thermocouple in a facial mask [90] and consisted of relative temperature over time.

For patients in group B the Real Time Position Management (RPM) system (Varian Medical systems) was used to track and record the respiratory traces both for reconstruction of 4DCT scans and for the coaching study (IV). The RPM system consists of a marker box with two reflective markers and an infrared camera interfaced to a computer. The RPM software installed on the computer records the traces of the box position via the reflective markers. The marker box was placed on the lower chest or upper abdomen and stabilised with bolus and adhesive tape to ensure an unambiguous presentation of the breathing phases.

Irregular breathing can cause artefacts in the 4DCT images and the breathing during acquisition of the 4DCT scans was analyzed using MATLAB. The breathing signal amplitude was defined as the breathing signal peak-to-peak displacement: For each breathing cycle an exhale point was defined as the 5% fractile of the box positions and an inhale point was defined as the 95% fractile of the box positions. The breathing signal amplitude was calculated as the distance between the inhale and the exhale point. The method is thoroughly described in [3]. As a measure of the variation of breathing signal amplitude, the SD of the breathing signal peak-to-peak displacement was found for each patient.

Breathing signal period was found as the time interval between two consecutive end-inspiration peaks. Mean and SD of the breathing signal periods recorded during 4DCT acquisition was calculated for each patient.

For study II and III only the breathing recorded during beam-on scan time was analyzed and the following linear regression analyzes were made: SD of breathing signal amplitude versus CV_{GTV} (II) and SD of breathing signal period versus CV_{GTV} (II, III).

From study IV the 120 s free breathing signal and the first 120 s of the two coached breathing signals from the reference day were analyzed and compared regarding variations in breathing signal amplitude and breathing signal period. For each volunteer the breathing signal amplitude of the two coached breathing signals were compared to the breathing signal amplitude of free breathing. The SD of breathing signal amplitude and period for the two coached breathings were compared to the SD of breathing signal amplitude and period for free breathing using a Wilcoxon paired signed rank tests (two-sided level of significance $p < 0.05$).

We evaluated if one of the two coaching approaches gave a less variable breathing pattern than the other and the SD of breathing signal amplitude of the two coaching approaches were compared.

STATISTICS

The present thesis is based on four separate original articles. Both parametric and non-parametric statistics were used. Parametric statistics were used when data or residuals (in case of correlations) were considered approximately Gaussian distributed. Where data were not considered Gaussian or in cases of uncertainty non-parametric tests were preferred.

In study I comparison between paired samples, e.g. variations of radiologists and oncologists, was performed using a paired student's t-test, with a two-sided level of significance, $p < 0.05$. For comparisons of independent samples, e.g. between tumours with and without pleural contact, an unpaired T-test with a two-sided level of significance, $p < 0.05$ was used. All correlations were calculated as linear regression analyzes with calculation of a Pearson product-moment correlation coefficient (Pearson correlation coefficient, r) and 95% confidence intervals (95%CI).

To improve the coherence and facilitate comparison some of the statistic analyzes from study II and III have been recomputed. Originally parametric statistics were used in study II and non parametric statistics were used in study III to compute the correlations between GTV size deviations and tumour motion, as well as between GTV size variations and breathing signal variations. The computation of correlations from study III was redone using linear regression with calculation of a Pearson correlation coefficient as in study II. The residuals of the linear regression computation were estimated to be approximately Gaussian distributed. The direct comparison between GTV sizes in study III was done using non-parametric statistics, i.e. Wilcoxon paired rank test was used (level of significance two-sided $p < 0.05$). In study IV a student's t-test (two-sided level of significance, $p < 0.05$) was used to compare breathing cycle amplitudes and a Wilcoxon paired signed rank test (two-sided level of significance, $p < 0.05$) was used for comparisons of SDs of breathing signal period and amplitude. Both the web site "VassarStats: Web Site for Statistical Computation" [91] and the SPSS Statistics program version 17.0 were used for statistical computations.

RESULTS

Inter-observer delineation variation (I)

Table 1 lists tumour size and position for all patients included in study I. Eighteen of the tumours were located in the upper and middle lobes and eight tumours were located in the lower lobes. The tumours were generally small, although one of tumour had a diameter of 7 cm (despite the recommendation of the local clinical guideline prescribes that only tumours up to 6 cm in diameter should be treated with SBRT). Approximately a third of the tumours had pleural contact.

Table 1 Tumour characteristics (study I)

Tumour localization	RUL	9
	LUL	8
	RML	1
	RLL	3
	LLL	5
Tumour diameter [cm]	Median (range)	3.25 (0.8 – 7.0)
Tumour volume [cm^3]	Median (range)	13.0 (0.3 – 60.4)
Pleural contact		9
Diagnosis	Early stage NSCLC	24
	Lung metastases	2

RUL: right upper lobe, LUL: left upper lobe, RML: right middle lobe, RLL: right lower lobe, LLL: left lower lobe, NSCLC: Non-Small Cell Lung Cancer

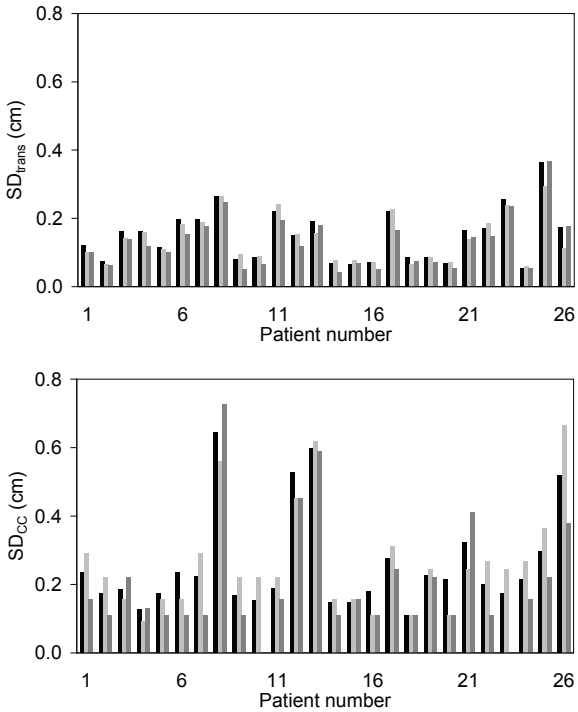

Figure 4

The tumour specific inter-observer delineation uncertainty in the transversal plane (SDtrans) and in the cranio-caudal plane (SDcc) for each tumour. The ordinal axis represents tumour number. All observers (■), radiologist (■) and oncologist (■).

SD_{trans} and SD_{cc} for all observers, radiologists and oncologists respectively are shown for all patients in figure 4 and results are shown in table 2. For tumour number 10 and 23 the tumour specific SDcc for the radiologists was 0 as all the radiologists had drawn the first and last contours in the same slices. The patient specific SD^{cc} was significantly larger than the patient specific SD^{trans} ($p < 0.0001$) being consistent with the anisotropic spatial resolution of the CT scan and the lack of possibility to delineate between slices in the sagital and coronal planes.

Table 1 Overall Results (study I)

	All observers	Radiologists	Oncologists
SD_{trans}:			
Mean [cm]	0.15	0.14	0.13
SD [cm]	0.08	0.07	0.08
Range [cm]	0.05 – 0.36	0.06 – 0.29	0.04 – 0.37
SD_{cc}:			
Mean [cm]	0.26	0.27	0.20
SD [cm]	0.15	0.15	0.17
Range [cm]	0.11 – 0.64	0.09 – 0.67	0.00 – 0.73
CI:			
Mean [cm]	0.72	0.68	0.75
SD [cm]	0.09	0.11	0.09
Range [cm]	0.56 – 0.87	0.47 – 0.88	0.59 – 0.90

SD: standard deviation, SD_{trans}: standard deviation of inter-observer delineation variation in the transversal plane, SD_{cc}: standard deviation of inter-observer delineation variation in the cranio-caudal direction, CI: concordance index calculated as a mean of all pair wise combinations of observers per tumour.

There was a significant but rather weak linear correlation between the patient specific SD_{trans} and SD_{cc}, r = 0.42 (0.04 - 0.69), implying that the larger the inter-observer delineation variation in the transversal plane the larger the inter-observer delineation variation in the CC plane. There was a significant correlation between SD_{trans} and tumour volume (r = 0.48, 95%CI 0.12 – 0.73), but not between SD_{cc} and tumour volume.

The mean absolute volume deviation between largest and smallest GTV was 6.4 cm3 (SD 6.0 cm3) ranging from 0.3 to 18.3 cm^3. The mean of the relative tumour specific volume deviations between largest and smallest GTV delineations was 41 % (SD 18 %) ranging from 14 % to 74 %. The reasons for the very large relative deviations is that tumour volumes generally were small, e.g. the tumour with the largest relative deviation was the smallest in the in the study measuring only 0.3 cm_3.

Figure 5 shows examples of tumours with large and small variations of contours in the transversal plane. For the tumour with the largest inter-observer delineation variation in the transversal plane (figure 5, left) there is a lack of concordance between the observers regarding an anatomical structure regarded by one of the observers as tumour and not by the rest of the observers possibly because of the lack of indication of PET positivity.

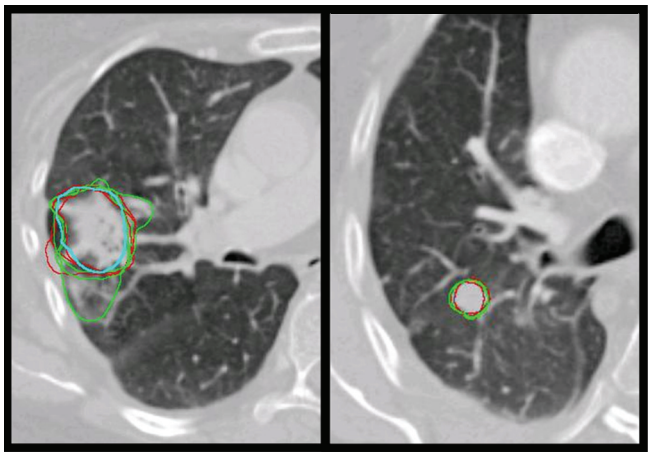

Figure 5

Left image: transversal view with contours of the tumour with the largest inter-observer delineation variation in the transversal plane (SD_{trans} was 0.36 cm and tumour volume was 16.3 cm^3). Right image: transversal views with contours of a tumour with a small inter-observer delineation variation in the transversal plane. (SD_{trans} was 0.07 cm and tumour volume was 1.5 cm^3). Radiologist's contours are red, oncologist's contours are green and the rough PET contour is blue.

Figure 6 shows examples of tumours with large and small variations of contours in the CC-direction. For all the three tumours imaged in figure 6 there was lack of concordance between the rough PET contour and the GTV contours stressing that PET was primarily used as a pointer and not to define the edge of the tumour.

Nine tumours had pleural contact and the mean SD_{trans} for this group was 0.19 cm (SD 0.07 cm). For the 17 tumours without pleural contact the SD_{trans} was 0.13 cm (SD 0.08 cm). The difference was significant (p = 0.032). There was no significant difference in SD_{cc} or CI between tumours with and without pleural contact.

The SD_{cc} was significantly larger for radiologists than for oncologists (p = 0.01). There was no difference for SD_{trans}. CI was significantly larger for the oncologists than for the radiologists ($p < 0.0001$).

We found a significant although weak correlation between tumour volume and CI (r = 0.39, 0.01 – 0.68), e.g. the larger the tumour the larger the CI.

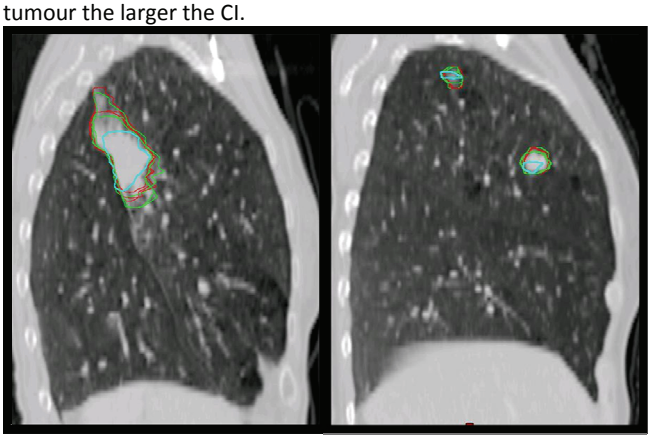

Figure 6

Left image: sagital views with contours of the tumour with the second largest inter-observer delineation variation in the cranio-caudal direction (SD_{cc} was 0.62 cm and tumour volume was 19.7 cm^3). Right image: sagital views with contours of two tumours in the right lung (the patient had three tumours). The caudal tumour had a small inter-observer delineation variation in the cranio-caudal direction, SD_{cc} being 0.11 cm (SD_{trans} was 0.09 cm and tumour volume was 0.7 cm^3). The cranial tumour in the right image had a SD_{cc} of 0.23 cm (SD_{trans} was 0.09 cm and tumour volume was 2.1 cm^3). Radiologist's contours are red, oncologist's contours are green and the rough PET contour is blue.

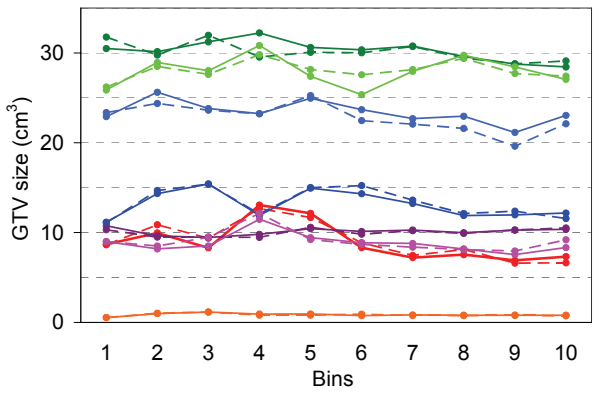

Figure 7

GTV size of all bins throughout the 4DCT scans of patients in group A. Each patient has a different colour. Initial delineations are in solid lines, re-delineations in dashed lines.

Intra-session delineation variation (II)

In study II the GTV contours in all bins were re-delineated for the eight patients with amplitude-binned 4DCT scans (group A). The initially delineated and re-delineated GTV sizes are plotted in figure 7. Each of the eight patients has a different colour. The initial delineations are marked in solid lines and the re-delineations are marked in punctuated lines.

By visual evaluation there seems to be no clear systematic difference between the GTV sizes resulting from the two delineations. The mean of the relative deviation between the initially delineated and re-delineated GTV sizes was −0.2% (SD 5.32%). A volume difference of 10.6% (2SD) was set to represent a threshold for deviation in GTV size considered to be caused by delineation variation in this study.

GTV variation in 4DCT (II, III)

For tumours analyzed in study II and III, table 3 lists tumour location, tumour motion in three directions, median (range) of mean of GTV sizes throughout the 4DCT scans, median (range) of the ranges of GTV sizes throughout the 4DCT scans, and median (range) of CV_{GTV}.

From study II the maximum deviations from the reference end-expiration GTV size (Dev_{max}) are listed also in table 3. It is noticeable that the group B tumours from study II were larger and also had larger tumour motion than the tumours in group A and in study III, as the group II patients were screened to have a tumour motion exceeding 0.5 cm and had more advanced tumours as previously described (see methods section).

Table 3 Tumour characteristics and GTV variations in 4DCT

	Study II		Study III
	Group A	**Group B**	**All**
Tumour location			
RUL	2	4	15
LUL	2	0	11
RML	0	1	2
RLL	2	6	11
LLL	2	1	7
Tumour motion [cm]			
LR	0.1 (0.1 – 0.3)	0.2 (0.1 – 1.0)	0.1 (0.0 – 0.4)
AP	0.3 (0.1 – 0.8)	0.4 (0.1 – 0.9)	0.2 (0.1 – 0.7)
CC	0.6 (0.2 – 1.0)	1.3 (0.2 – 3.2)	0.4 (0.0 – 2.4)
Mean GTV size [cm^3]	11.6 (0.9 – 30.3)	32.2 (1.6 – 176)	5.2 (0.2 – 58.9)
Range GTV size [cm^3]	4.1 (1.3 – 6.2)	5.3 (0.4 – 15.6)	0.9 (0.1 – 11.6)
CV_{GTV} [%]	8.7 (3.7 – 23.8)	6.6 (1.3 – 25.7)	6.3 (1.7 – 24.5)
Dev_{max} [%]	20.2 (-8.7 – 78.6)	11.5 (-22.1 – 90.8)	-

Median (range) values are listed. RUL: right upper lobe, LUL: left upper lobe, RML: right middle lobe, RLL: right lower lobe, LLL: left lower lobe, LR: left-right, AP: anterior-posterior, CC: cranio-caudal, CV_{GTV}: coefficient of variation of GTV size throughout the 4DCT, Dev_{max}: maximal value of numeric deviation of GTV sizes throughout a 4DCT from the reference volume.

For 16 out of the 20 tumours in study II Dev_{max} was larger than what could be accounted for by intra-session delineation variation.

In figure 8 the relative deviation from the reference GTV_{exp} for all bins is plotted. Only the tumours with GTV deviations larger than what could be expected from intra-session delineation error are plotted: seven tumours from group A and nine tumours from group B. By visual evaluation it is noticeable that for some bins very large deviations in GTV sizes were present especially around the end-inspiration bin. The smallest deviations were present in the bins of the expiratory phase.

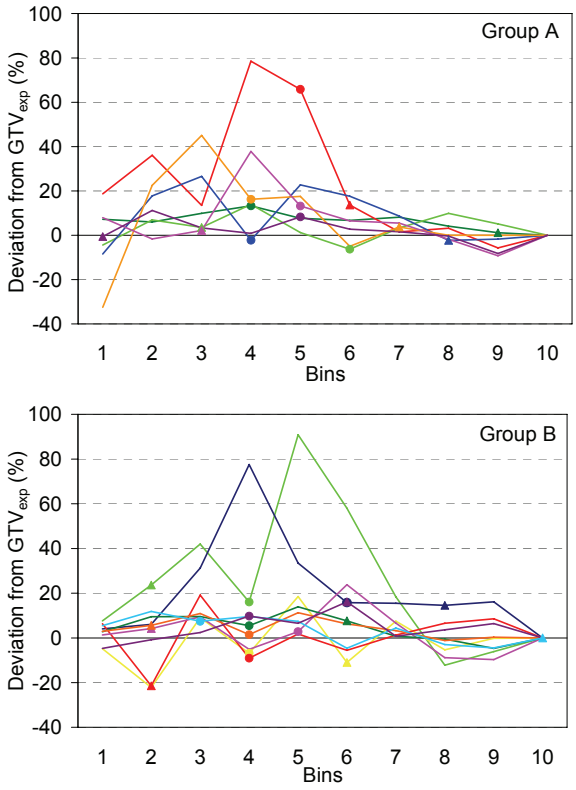

Figure 8
The relative deviation from the reference GTV_{exp} for all bins is plotted for group A and B. Only tumours where GTV deviations were larger than what could be expected from intra-session delineation error are plotted. For all patients bin 10 is end-expiration (GTV_{exp}). The end-inspiration bin is marked with (●) and the mid-ventilation bin is marked with (▲). Each patient has a different colour.

Figure 9 shows sagital reconstructions from the 4DCT scans of the patient, from group A and Group B respectively, with the largest Dev_{max}. Artefacts are visible in both the tumour and diaphragm regions.

A significant negative correlation was found between GTV_{mean} and CV_{GTV} for group A, i.e. the smaller the tumour the larger the variation in GTV size throughout the 4DCT (r = −0.71, 95%CI −0.94 to −0.004) while the correlation did not reach statistical significance for group B (r = −0.57, 95%CI −0.862 to 0.002). In study III the correlation between GTV_{mean} and CV_{GTV} was significant (r = −0.55, 95%CI −0.73 to −0.31).

Table 4 Overall absolute and relative deviations of GTV_{3D}, GTV_{MidV}, GTV_{Insp} and GTV_{Exp} from the reference GTV_{BH} (study III).

	Deviation from GTV_{BH} [cm3]			Deviation from GTV_{BH} [%]		
	Median	Min.	Max.	Median	Min.	Max.
GTV_{3D}	0.3	−3.3	30.3	6.1	−36.0	120
GTV_{MidV}	0.2	−2.9	10.3	6.3	−47.2	120
GTV_{Insp}	0.3	−2.8	6.1	7.3	−46.7	80
GTV_{Exp}	0.3	−2.2	4.7	5.2	−50.3	100

GTV_{BH}: GTV size in breath-hold CT, GTV_{MidV}: GTV size in the midventilation bin of the 4DCT, GTV_{Insp}: GTV size in the end-inspiration bin of the 4DCT, GTV_{Exp}: GTV size in the end-expiration bin of the 4DCT

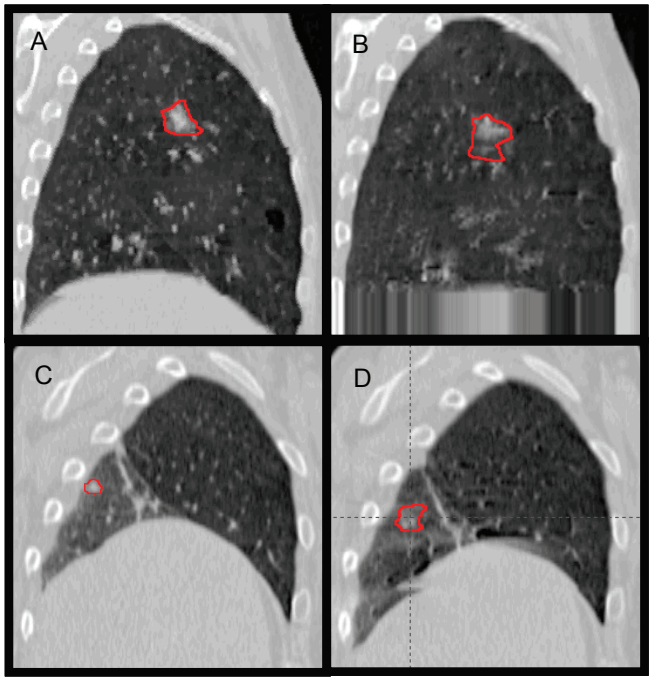

Figure 9
Sagital reconstructions from the 4DCT scans of the patients, from group A and group B respectively with the largest Dev_{max}: (A) End-expiration bin for patient 3 in group A. GTV size was 7.3 cm^3. (B) Bin 4 for patient 3 in group A, where deviation in GTV size was largest. GTV size was 13.1 cm^3. Several artefacts are seen in the tumour area and also in the diaphragm area and thoracic wall. The blurring in diaphragmatic area is caused by interpolation caused by missing images in the bin. (C) End-expiration bin for patient 2 in group B. GTV size was 1.3 cm^3. (D) Bin 5 for patient 2 in group B where deviation in GTV size was largest. GTV size was 2.5 cm^3.

In study III the median (range) GTV sizes were GTV_{BH}: 4.9 cm^3 (0.1 to 53.3 cm^3), GTV_{3D} 5.3 cm^3 (0.2 - 64.9 cm^3), GTV_{MidV} 5.6 cm^3 (0.2-59.7 cm^3), GTV_{Insp} 4.9 cm^3 (0.2 – 59.3 cm^3), and GTV_{Exp} 5.3 cm3 (0.2 – 58.0 cm^3).

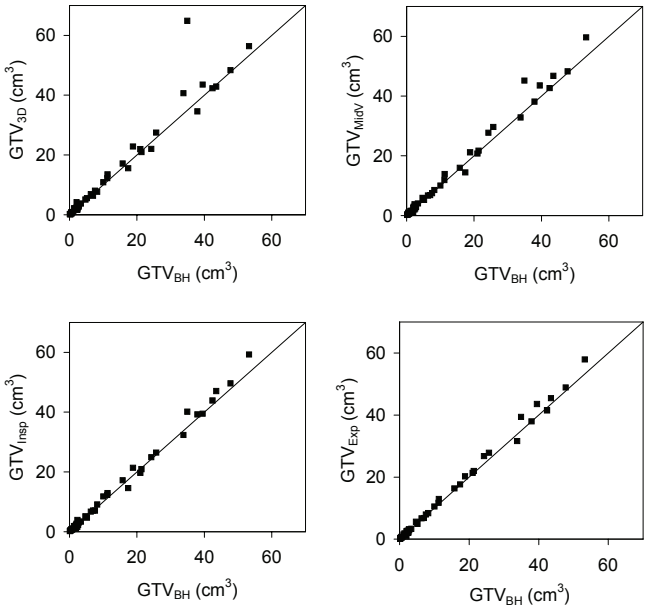

Figure 10
Reference breathhold CT GTV size (GTV_{BH}) plotted against A) GTV size in 3DCT (GTV_{3D}), B) midventilation GTV size (GTV_{MidV}), C) end-inspiration GTV size (GTV_{Insp}) and D end-expiration GTV size (GTV_{Exp}).

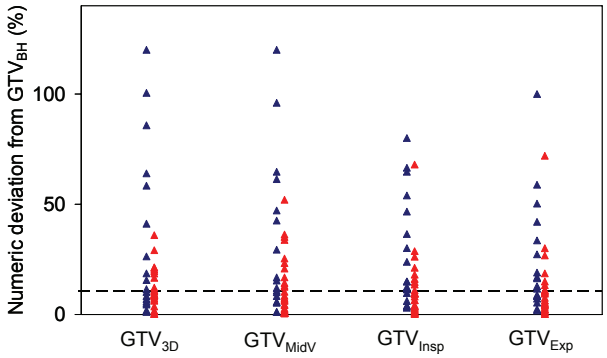

Figure 11
Plot of the relative numeric deviations from the reference GTV_{BH} size for 3D- and 4DCT GTVs. Tumours in the lower lobes are in blue colour and tumours in the middle and upper lobes are in red colour. The punctuated line indicates the intra-session delineation variation of 10.6 % as found in study II.

In figure 10 the reference GTV_{BH} is plotted against GTV_{3D}, GTV_{MidV}, GTV_{Insp} and GTV_{Exp} respectively. By visual inspection GTV_{Exp} and GTV_{Insp} seems closest to the reference GTV_{BH}. There was a significant difference between the GTV_{3D} and GTV_{BH} ($p = 0.017$), between GTV_{MidV} and GTV_{BH} ($p = 0.0002$), between GTV_{Insp} and GTV_{BH} ($p = 0.003$), and between GTV_{Exp} and GTV_{BH} ($p = 0.0005$).

Table 4 shows the overall absolute and relative deviations of GTV_{3D}, GTV_{MidV}, GTV_{Insp} and GTV_{Exp} from the reference GTV_{BH}. For most patients the deviations were small but for a few patients the deviations were very large, up to 30 cm^3.

In figure 11 the relative numeric deviations from the reference GTV_{BH} size are plotted for 3D- and 4DCT GTVs. The threshold from study II indicating intra-session delineation variation is marked with a punctuated line. The largest deviations were seen for tumours in the lower lobes, but also tumours from the upper lobes had deviations exceeding the intra-session delineation variation.

Figure 12 shows coronal CT reconstructions of two patients with very large deviations in GTV size between 3DCT, MidV and BHCT scans.

Artefacts and tumour motion (II, III)

In two of the studies correlation analyzes between tumour motion in the CC direction and deviations in GTV sizes were computed. In both studies a significant linear correlation between CVGTV and tumour motion in the CC direction was found, i.e. the larger the tumour motion the larger the variation in GTV size throughout the 4DCT. In study II the two groups were analyzed separately: for group A the Pearson correlation coefficient was 0.78 (95%CI 0.17 - 0.96) and for group B the Pearson correlation coefficient was 0.70 (95%CI 0.21 - 0.91). In study III, where the proportion of tumours with small tumour motion in the CC direction was larger than in study II, the Pearson correlation coefficient was 0.31 (95%CI 0.03 - 0.55).

In study III there was a vague but significant linear correlation between the relative numeric deviations from the reference GTV_{BH} and CC tumour motion for GTV3D ($r = 0.37$, 95%CI 0.09 – 0.60) and GTV_{MidV} ($r = 0.29$, 95%CI 0.002 – 0.54) respectively. There was no significant linear correlation between the relative numeric deviations from the reference GTV_{BH} and CC tumour motion for GTV_{Insp} and GTV_{Exp}.

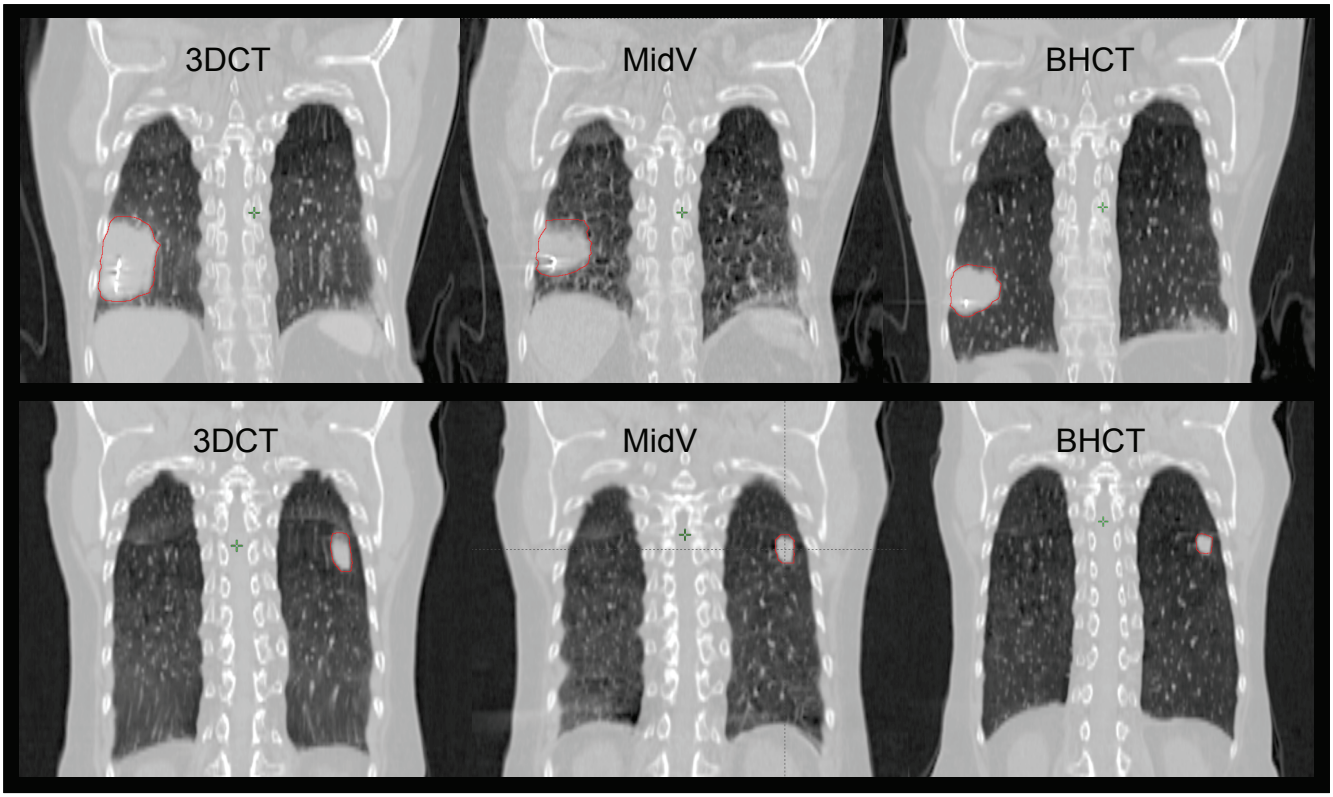

Figure 12
Coronal reconstructions of different CT scans of two patients with large deviations in GTV between scans. The upper row shows coronal reconstructions of a patient with a tumour in the right lower lobe: conventional CT (left), midventilation bin (middle) and breathhold CT (right) of the same patient. GTV size was 64.9 cm^3, 45.2 cm^3 and 34.9 cm^3, respectively, and the CC tumour motion was 2.4 cm. The patient had an implanted gold marker. The lower row shows coronal reconstructions of a patient with an apical tumour in the left lower lobe; conventional CT (left), midventilation bin (middle) and breathhold CT (right). GTV size was 4.2 cm^3, 3.0 cm^3 and 2.1 cm^3 respectively and CC tumour motion was 0.6 cm.

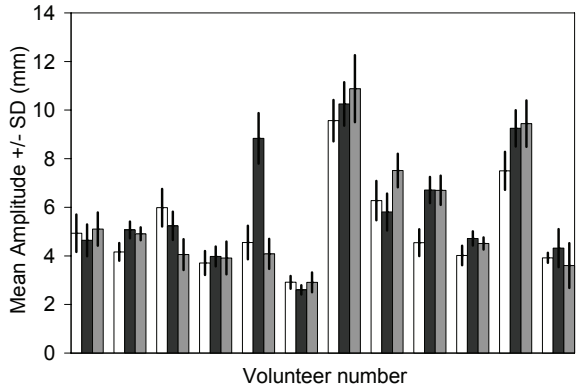

Figure 13
Mean and SD of the breathing cycle amplitude distribution for free breathing (□), coaching 1 (■) and coaching 2 (■) on the first day for the 12 volunteers.

Artefacts and breathing signal variations (II, III)

In group A and B the median scan time was 360 and 100 seconds, respectively. In group A the median SD of the breathing signal peak-to-peak displacement of the breath temperature was in relative units 0.17 (range 0.13 - 0.23). In group B the median SD of the breathing signal peak-to-peak displacement of the external marker block was 0.16 cm (range 0.05 - 0.40).

We found no significant linear correlation between SD of breathing signal peak-to-peak displacement and CV_{GTV} for neither group A or B.

The median SD of the breathing signal period was 0.35 seconds (range 0.25 – 0.50) for group A and 0.52 seconds (range 0.16 – 1.12) for group B. We found no linear correlation between the SD of breathing signal period and CV_{GTV} for neither group A or B.

In study III the mean breathing signal period ranged from 2.1 to 6.1 seconds (s) with a median of 3.3 s between patients. SD of breathing signal period varied from 0.1 to 1.2 s with a median of 0.6 s. The SD of breathing signal period was significantly correlated to CV_{GTV} ($r = 0.40$, $p = 0.005$), i.e. the larger the variation in breathing signal period the larger the variation in GTV size throughout the 4DCT.

Respiratory Coaching (IV)

The characteristics of the volunteers included in study IV are shown in Table 5. One of the volunteers (age 62, former smoker, no pulmonary disease) was excluded as the volunteer was not able to follow the audio coaching at all. The data from the remaining 12 volunteers were analyzed.

Table 5 Characteristics of the volunteers (study VI)

Age (years)	46 (26 - 64)*
Gender (F/M)	11 / 2
Smoking status (smokers / former / never)	3 / 4 / 6
Respiratory disorders	COPD 1 Asthma 1

COPD: Chronic obstructive pulmonary disease, median (range) values are listed.

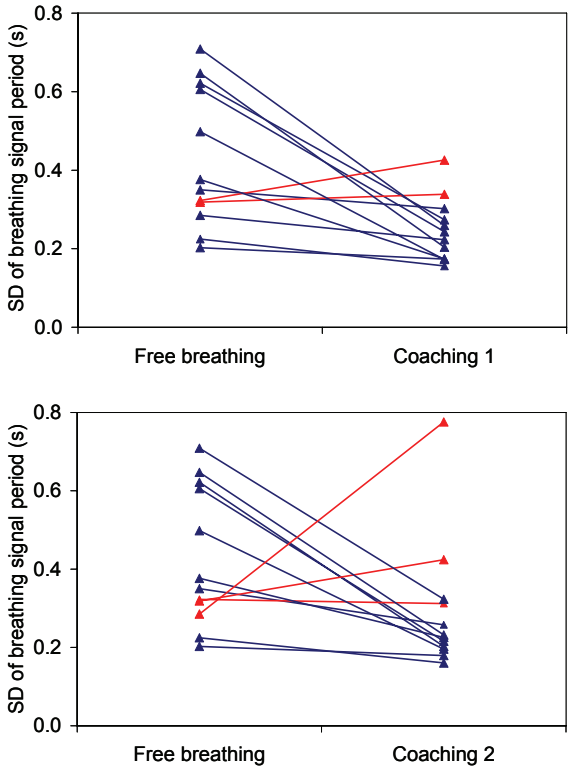

Figure 14
The SD of the breathing signal amplitude for free breathing plotted against the SD of the breathing signal amplitude for coaching 1 and coaching 2 respectively. Blue colour indicates a decrease in SD between free breathing and coaching while red colour indicates an increase in SD between free breathing and coaching.

Figure 13 shows the mean and SD of the breathing signal amplitude in free breathing, coaching 1 and coaching 2 on the reference day for the 12 volunteers. The magnitude of the changes in breathing cycle amplitude was small although significant for the majority of volunteers.

With the first coaching approach the breathing signal amplitude increased significantly for seven volunteers and decreased significantly for two volunteers compared to free breathing (p values between <0.0001 and 0.0156). With the second coaching approach the breathing signal amplitude increased significantly for six volunteers and decreased significantly for two volunteers compared to free breathing ($p<0.0001$ – 0.0237).

Figure 14 compares the SD of breathing signal period for free breathing to SD of breathing signal period for coaching 1 and coaching 2 respectively. There was an increase in SD of the breathing signal period for two and a decrease for ten of the 12 volunteers with coaching 1. With coaching 2 there was an increase in SD of the breathing signal period for three and a decrease for nine of the volunteers. The overall decrease in SD of breathing signal period for coaching 1 compared to free breathing was significant ($p = 0.013$) while this was not the case for coaching 2 ($p = 0.088$).

Figure 15 compares the SD of the breathing signal amplitude on day 1 for free breathing, coaching 1 and coaching 2 respectively.

There was an increase in SD of the breathing signal amplitude for three and a decrease for nine of the 12 volunteers with coach 1. With coach 2 there was an increase in SD of the breathing signal amplitude for six and a decrease for six of the volunteers.

Overall there was no significant change in SD of the breathing signal amplitude for either coaching approach compared to free breathing.

At the reference session there was no significant difference between the SD of breathing signal period ($p = 0.49$) or amplitude ($p = 0.25$) of the two coaching approaches. Three of the volunteers wanted no change in the in- and expiration intervals for coaching 2 compared to coaching 1, the rest of the volunteers wanted to extend the in- or expiration interval.

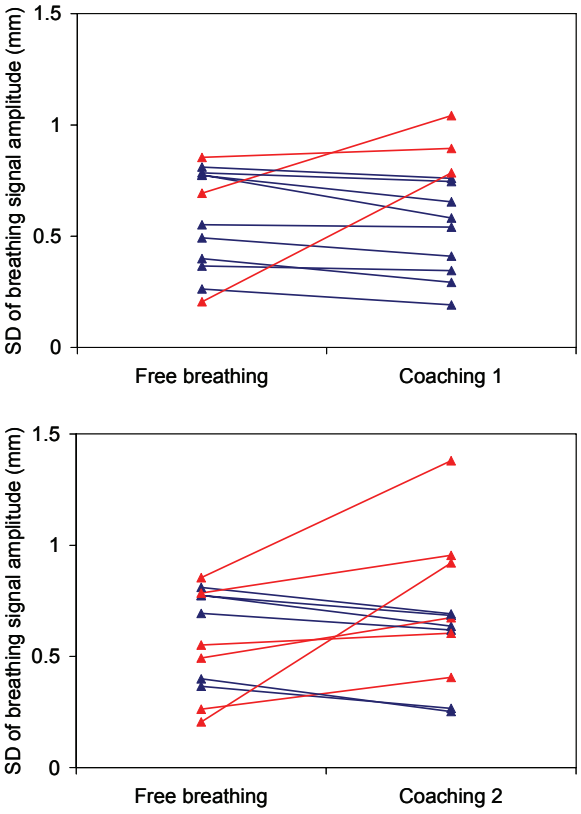

Figure 15
The SD of breathing signal period for free breathing plotted against the SD of breathing signal period for coaching 1 and coaching 2 respectively. Blue colour indicates a decrease in SD between free breathing and coaching while red colour indicates an increase in SD between free breathing and coaching.

DISCUSSION

The studies in the present thesis showed that inter-observer delineation uncertainties were very small for peripheral lung tumours although larger in the CC direction compared to the transversal plane (study I). Artefacts in imaging significantly impacted the size of the delineated GTV and large tumour motion was correlated to imaging artefacts (study II and III). In study III a correlation to irregular breathing was also demonstrated. It was also shown that respiratory audio coaching could increase the regularity of the breathing frequency but had a significant although small impact on breathing amplitude most often increasing the amplitude. An advantage in studying peripheral lung tumours, in relation to uncertainties in target definition, is the large difference in density between tumour and surrounding lung tissue. It makes the tumours easy to define and makes the peripheral lung tumours suitable for analyzing the impact of artefacts in imaging.

Delineation uncertainty

Study II differs from earlier studies [38,40,47,92] examining inter-observer delineation uncertainty by two characteristics. First, it was designed as a cross-sectional study analyzing the inter-observer delineation variation in a well defined group of patients with peripheral lung tumours referred for SBRT. Secondly, the inter-observer variation in the CC direction was analyzed separately from the transversal plane. The rationale for the use of this method was that CT scans has anisotropic image resolution: They are constructed of slices and the inter-observer variation in the CC direction will directly depend on the slice thickness.

A low inter-observer variation of 0.15 cm in the transversal plane and 0.26 cm in the CC direction at the level of one standard deviation was found. The variation was small compared to previous studies examining more heterogeneous tumours: Steenbakkers et al. [38] and Fitton et al. [47] analyzed 22 locally advanced tumours, delineated by 11 experienced radiation oncologists from five different institutions. They analyzed each anatomic region separately and thus also the part of the tumours bordering lung tissue and the thoracic wall. They included PET information, but not contrast enhancement, and had a detailed protocol for delineation. They found an inter-observer variation of 0.33 cm for tumour regions bordering lung tissue and 0.37 cm for tumour regions bordering the chest wall (SD useable for margin calculations [1,91]). Looking only at the primary tumours surrounded by lung or visceral pleura the inter-observer variation was 0.3 cm.

Several other investigators have studied inter-observer variation in GTV delineations for lung cancer [37,39,40,92,93]. All have included a broad selection of locally advanced cancers and only a few have included $T_{1\text{-}2}N_0M_0$ tumours. All studies found large overall delineation variations and small CI values which were to be expected, especially due to the inclusion of mediastinal tumours where tumour and surrounding tissue densities are similar, but also due to the lack of a delineation protocol or PET information in the majority of studies.

The uniform use of the PET information in study II probably helped to minimize variation, as did the fact that the observers (oncologists and the radiologists) in their daily clinical work cooperate in the delineation of GTVs, which may tend to produce a common view in the delineation of lung tumours. Nevertheless, a higher concordance was seen among oncologists than among radiologists. This finding was primarily driven by uncertainties in CC direction as there was a significant difference between radiologists and oncologists in this direction and not in the transversal plane.

Giraud et al. [40] analyzed delineations of stage I – IIIB NSCLC by nine radiation oncologist and eight radiologists from five centres. They found that the oncologists drew a significantly larger volume but found no difference in CI for radiologist versus oncologist.

The nature of delineation uncertainties is not simple and can be looked upon as being a composite of two fundamentally different types of variation. First a presumably random variation in the accuracy of where exactly the observers draw the line using the software and equipment at hand. These uncertainties will follow a normal distribution and methods like the one described in study I will be useful to determine the magnitude of the variation. This part of the delineation variation is inevitable and has to be taken into account by the addition of a margin. Secondly, a variation caused by the observers' decision on whether to include or not include certain anatomic structures in the GTV, is present. This variation will most probably not follow a normal distribution and is therefore not well represented by a standard deviation.

The best way to minimize these systematic variations is to ensure the best possible education and instructions for the observers and to optimize imaging strategies for GTV delineation purposes. In a recent study by van Loon et al. [94], the GTV was delineated on preoperative CT scans and PET scans, and were subsequently correlated to the pathology specimens of patients undergoing lobectomy using deformable registration. Future refinement of this method [12,95] could facilitate studies using pathology specimens as reference for GTV, providing further knowledge on the association between CT, PET and pathology. Furthermore, the delineation work performed by the clinicians should always be evaluated and further developed through thorough follow-up of patients and analysis of the exact location of recurrences. For peripheral lung tumours included in study II the inter-observer delineation uncertainty in the transversal plane is probably dominated by the first type of uncertainty which is probably quite well described using SDs. The inter-observer delineation uncertainty in CC-direction is probably more influenced by the second type of variation where observers take different decisions of whether to delineate in an additional slice or not. In the present study the agreement in the CC-direction was better between oncologists than between radiologists.

A limitation to the present, and other studies of inter-observer delineation variation, is the lack of consensus of metrics which makes quantitative comparisons of data difficult. Hannah et al. have reviewed the methods of studies on target volume definition [96]. They found 28 paper concerning lung cancer looking at a wide variety of parameters, e.g. GTV, CTV and PTV. Twenty-four of the papers reported simple volume comparisons, seven reported CIs and only two provided volume edge analysis (SDs) [47,72]. The method used in study I utilizes a CoV as reference point which is suitable for rounded tumours, such as peripheral lung tumours, but not suitable for very concavely shaped volumes, where the CoV will be placed outside the volume. The fact that the result to a high degree depends on imaging protocols and qualifications of the observers can make the extrapolation of our results to other institutions difficult.

A rather important limitation to study I is that it is based on 3DCT scans and not on 4D technology. It cannot readily be assumed that these results are applicable to 4D technology or CT scans acquired using breathhold techniques. The inter-observer delineation variation in the present study will probably be a reasonable estimate of the inter-observer delineation variation of the midventilation phase of a 4DCT scan [53], BHCT scans may have even smaller delineation variation as motion artefacts are less likely [97]. These hypotheses obviously need confirmation from future studies.

Imaging artefacts

Both study II and III focus on the impact of image artefacts on delineated GTV size. Study II can be considered as a pilot study demonstrating the presence and impact of artefacts in both amplitude and phase binned 4DCT scans. In study III a cross-sectional design was used to demonstrate the prevalence in a well defined patient group with BHCT scans acquired for reference volumes. Deviations in GTV size exceeding what could be expected from delineation variation was found in almost half the included patients. The largest deviations were found for the 3DCT and midventilation bins. For the majority of patients the differences were small but for a few patients the differences were large and without doubt of clinical relevance. In both Study II and III a significant correlation was found between tumour motion in the CC direction and CV of GTV size, although rather weak in study III. This is probably due to the larger proportion of tumours with small movements in the unselected cohort, where delineation uncertainty plays a proportionally larger role.

Previous studies have analyzed and documented the presence of artefacts in both 3D- and 4DCT, performed in either smaller or more heterogeneous patient groups or based on phantom experiments. Our clinical approach with analysis of the delineated GTV, the comparison to a reference BHCT GTV, and the cross-sectional design in study III makes the results comprehensible and differentiable from previous studies.

A large study by Yamamoto et al. analyzed phase-binned cine-mode 4DCT scans of 50 patients, with thoracic or abdominal tumours, and found visible artefacts in the diaphragm or heart in 90 % of the scans [23]. For six out of 20 patients with lung or mediastinal tumours visible artefacts were found in the images of the tumours.

Several phantom studies have studied 4DCT and artefacts: Nakamura et al. [98] found an increase in artefacts with increasing target velocity. Sarker et al. [99] performed a study using a setup with a virtual CT scanner and found volume variations increased with peak-to-peak target motion. Watkins et al. [100] found that presuming a consistent breathing pattern, artefacts due to intra phase motion could be predicted based on scanner settings, target motion, and breathing period, and suggested the incorporation of this patient specific uncertainty into margin calculations.

Several factors will impact the GTV size variations: Delineation uncertainty, tumour deformation due to breathing, and image artefacts.

Delineation uncertainty undoubtedly affected the GTV size variations, although the choice of peripheral lung tumours for examining the influence of artefacts on GTV size should ensure the smallest possible impact from delineation error. The delineation uncertainty (intra-session delineation variation) is estimated in study II and as illustrated by figure 11 it is reasonable to assume that artefacts do impact GTV size to an even larger extent than delineation error for many patients with peripheral lung tumours.

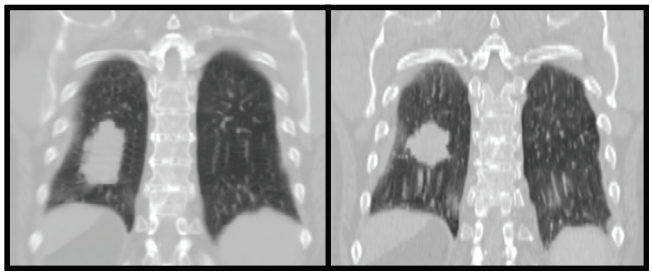

Figure 16
Coronal reconstructions of 3DCTs of a patient with a tumour in the right lower lobe; diagnostic conventional CT (left) and therapeutic conventional CT (right). The diagnostic CT scan was acquired two months before the therapeutic CT scan. The patient did not receive any anti-neoplastic treatment in between the two scans.

Although the median 3D- and 4DCT GTV sizes were significantly larger than the median reference GTV_{BH}, GTV sizes both larger and smaller than the reference GTV_{BH} were seen, indicating a random factor. This randomness is most likely primarily caused by delineation uncertainty, as the magnitude of the negative GTV size deviations are same as the magnitude the volume deviations caused by intra-session delineation uncertainty. However, in the

3DCT scans, the GTV size deviations can also be affected by the scanning process and depend on whether the tumour during the scan moved in the same or opposite direction of the scan direction [19,100]. Figure 16 shows an example of this randomness in GTV size in 3DCT scans, where the GTV in an earlier diagnostic CT scan is much larger than the GTV in the therapeutic PET/CT scan.

In both study II and III a significant negative correlation was found between GTV_{BH} and CV of GTV size throughout the 4DCT scans, i.e. the smaller GTV_{BH} the larger the CV. This is most probably caused by the larger surface/volume in small tumours making the partial projection- and volume effects relatively more evident as well as the relative impact of delineation uncertainties.

A drawback of using deviations in GTV size as an indicator of artefacts in 3D- and 4DCT scans is the roughness of the method. The prevalence and impact of artefacts will probably be underestimated as artefacts can cause deformation of the tumour image without changing the volume and/or the artefacts can be masked by delineation variations. An example from study II is shown in figure 17.

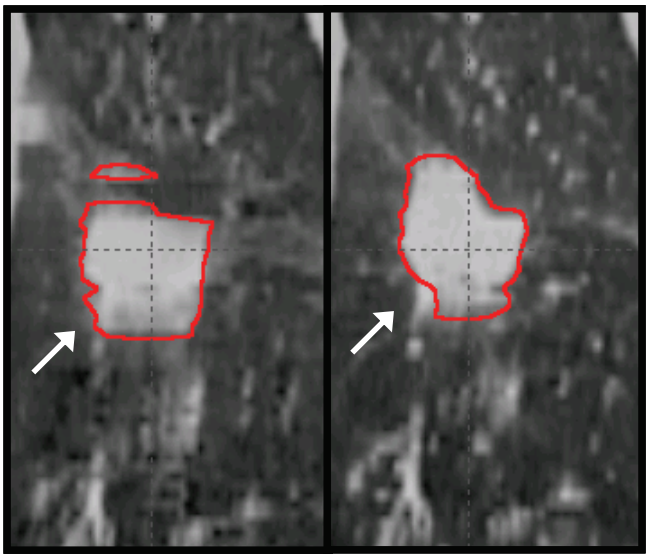

Figure 17
Reconstructed coronal views from two different bins of the 4DCT of a patient from group A. The GTV sizes in the two bins are almost the same. In bin 2 (left) GTV size was 30.1 cm3 and in bin 5 (right) GTV size was 30.6 cm3. Note both the artefact in bin 2 and the discrepancy in delineation, where a part of a vessel (arrow) is included in bin 2 but not in bin 5.

In neither study II nor III are the effect of potential stretching and compression of the tumours throughout the breathing phases in the different CT scans accounted for. In study III the GTV size from a voluntary inspiration breath hold scan was used as a reference. This holds a potential drawback of the study as tumours may stretch during deep inspiration yielding larger GTVs. Nevertheless the impact of tumour stretching can probably be estimated as small, compared to the variations caused by artefacts and delineation error: GTV_{BH} (in deep inspiration) actually resulted in the smallest target volumes. This suggests that breathing related tumour stretching was limited.

The issue of breathing related artefacts is not relevant for peripheral lung tumours only; it is merely easily detectable for this group of tumours. In the treatments of other patient groups, e.g. locally advanced lung cancer, breast cancer, liver cancer and lymphoma patients where tumours move with respiration, clinicians are also challenged by this problem.

Advanced radiotherapy techniques such as Intensity Modulated Radiotherapy (IMRT) make experimental techniques such as "Dose Painting" possible [101]. However, these technologies rely on precise and consistent imaging of target volumes as well as normal tissues. The usefulness of these techniques in lung cancer radiotherapy will be hampered by lack of accuracy in imaging and will depend on further developments in imaging techniques.

With the purpose of reducing artefacts, newer studies have examined combined phase and amplitude binning, as well as prospective binning methods for 4DCT with promising results [36,102-105]. However none of these methods are commercially available. Newer CT scanners with faster rotation time and larger collimation can also contribute to minimizing artefacts.

In recognition of that artefacts to some degree are inevitable a supplementary breathhold CT scan is recommended to provide a reference for tumour volume, especially when using the mid-ventilation approach for radiotherapy of lung tumours.

Respiratory coaching

The results with audio coaching are very dependent on the method used and the chosen rhythm of the audio prompts. The hypothesis in study IV was that by using the typical rhythm of the volunteers' free breathing the increase in breathing depth (increase in breathing signal amplitude) as seen in previous studies could be avoided [50].

Respiratory audio coaching improved breathing regularity for the majority of volunteers, but it also introduced a significant change of the breathing signal amplitude between free and coached breathing for most volunteers. The absolute difference was small for the majority of volunteers, but the relative changes could be relevant, as changes in breathing motion translate into similar changes in tumour motion [106,107]. No significant change in SD of breathing signal amplitude was found between free breathing and either of the two coaching approaches, i.e. the variability of the breathing signal amplitude was not improved by the audio coaching.

The purpose of respiratory coaching in the present study was to achieve a more regular breathing in order to decrease the risk of image artefacts, without increasing the amplitude as this would lead to larger tumour motion and thereby increase the risk of image artefacts because of larger residual motion within the 4DCT bins. Previous studies have examined the impact of audio coaching and have found that breathing regularity increases but breathing signal amplitude increases with audio coaching compared to free breathing [50,51,108,109]. To really optimize the patients' breathing during 4DCT acquisition of a 4DCT scan both the variations in breathing signal amplitude and period should be decreased. A sophisticated approach is to use audio-visual coaching to guide both the regularity and the amplitude of the breathing. Studies have documented the potential but encountered a feasibility problems since not all patients can comply with the techniques [109].

A new coaching approach using a bio-visual feedback mechanism is being examined at Stanford University [110,111] in a clinical setting with the purpose of minimizing artefacts in 4DCT scans.

The largest limitation of study IV was that breathing signals were acquired from volunteers and not from lung cancer patients and that no imaging was performed. The question whether coaching can help in minimizing artefacts and what the impact is on tumour motion can only be answered in patient trials acquiring 4DCT scans with and without applied coaching. In a study by

Haasbeek et al., audio coached and uncoached 4DCT scans were analyzed. They found that coaching significantly increased tumour motion, mainly in the CC direction [112].

Probably the most promising aspect of patient coaching for lung cancer radiotherapy is not in only in the planning situation and the need for artefact free imaging, but also to use coaching with the purpose of making the breathing more predictable and reproducible. The audiovisual biofeedback approach using a waveform and sound, as proposed by the Stanford group [110,111] may hold potential but needs to be proven useful in a clinical setting. This would facilitate the optimisation of new treatment options such as tumour tracking or gating as treatment options for patients with large tumour motion.

Another possible option is to use respiratory coaching to guide patients to deep inspiration breathhold during planning and treatment. This holds many promising aspects: reduced breathing related artefacts in the planning scan, safer application of IMRT techniques and "dose painting" with reduced risk of interplay effect [113], and geometrical advantage of the inflated lung with a decrease in normal tissue toxicity. Obviously, this presupposes that the patients are able to hold their breath for a minimum of time during treatment and imaging performed to confirm positioning and reproducibility of the breathhold.

CONCLUSION

In the present thesis uncertainties in GTV definition for radiotherapy of peripheral lung tumours were investigated. The inter-observer delineation variation determined in study I was very small although significantly larger in the CC direction compared to the transversal plane stressing that anisotropic margins should be applied. In study II GTV size variation larger than delineation variation could account for, was found in both amplitude and phase binned 4DCT scans indicating the presence of significant image artefacts. In Study III the choice of CT method significantly impacted the GTV size on average leading to an increase in GTV size when compared to the GTV size in a breathhold CT indicating the presence of artefacts. The differences were largest for 3DCT and the midventilation bin. Most differences were small but for a few patient very large differences were seen. The variations in GTV size were correlated to both tumour motion and breathing irregularity. It is recommended to acquire a supplementary breathhold CT scan as a reference for tumour volume when using the midventilation approach for radiotherapy of lung tumours.

With respiratory audio coaching it was possible to achieve a more stable breathing for a majority of volunteers but not without changing the amplitude of the breathing. The impact of respiratory coaching on image quality in 4DCT needs further investigation.

PERSPECTIVES

The trend toward more individualized treatment margins is the overall tendency within modern radiotherapy. It is facilitated by better and more available imaging, e.g. functional imaging and image guidance. With further individualized margins and treatment plans we hope to increase our chance of local control while decreasing treatment toxicity. In the present PhD thesis uncertainties regarding target definition for SBRT of peripheral lung tumours have been investigated. Many other systematic and random uncertainties in treatment delivery impact the treatment and are being intensively investigated with the purpose of designing more precise individualised margins [4,5,114]. These uncertainties must be taken into account when introducing and refining the highly individualized and conformal treatment plans which can now be delivered to patients. It is of most imperative importance, when changing the treatment, that thorough follow-up of all patients is ensured and results entered into databases. Morphological imaging, and probably also functional imaging in case of relapse, should be acquired together with regular registering of toxicity. This is the only way assure that we do not unintentionally increase the risk of relapse or toxicity by tailoring the treatment to the individual, using highly conformal techniques but not paying sufficient attention to the uncertainties in our techniques.

ACKNOWLEDGEMENTS

The studies were supported by grants from "The Danish Council for Independent Research in Medical Sciences", Arvid Nilssons Foundation, Astrid Thaysens Foundation and the Lundbeck Foundation Center for Interventional Research in Radiation Oncology (CIRRO).

ABBREVIATIONS

AP	Anterior-posterior direction
BHCT	Breathhold CT
CC	Cranio-caudal direction
CI	Concordance index
95%CI	95 % confidence interval
CT	Computer tomography
CTV	Clinical target volume
CV	Coefficient of variation (SD/mean)
CV_{GTV}	Coefficient of variation of GTV size throughout the 4DCT
CoV	Centre of volume
3DCT	Conventional CT
4DCT	Respiratory correlated CT
DEV_{max}	Maximal value of numeric deviation of GTV sizes throughout a 4DCT from the reference volume (GTV_{exp})
GTV	Gross tumour volume
GTV_{BH}	Size of gross tumour volume in breathhold CT
GTV_{3DCT}	Size of gross tumour volume in conventional CT
GTV_{exp}	Size of gross tumour volume in the expiration bin of the 4DCT
GTV_{insp}	Size of gross tumour volume in the inspiration bin of the 4DCT
GTV_{MidV}	Size of gross tumour volume in the midventila tion bin of the 4DCT
LLL	Left lower lung lobe
LUL	Left upper lung lobe
LR	Left-right direction
NSCLC	Non small-cell lung cancer
RUL	Right upper lung lobe
RML	Right middle lung lobe
RLL	Right lower lung lobe
PTV	Planning target volume
SBRT	Stereotactic body radiotherapy

REFERENCES

1. van Herk M. Errors and margins in radiotherapy. Semin Radiat Oncol 2004;14:52-64
2. Juhler-Nottrup T, Korreman SS, Pedersen AN, Persson GF, Aarup LR, Nystrom H et al. Interfractional changes in tumour volume and position during entire radiotherapy courses for lung cancer with respiratory gating and image guidance. Acta Oncol 2008;47:1406-13
3. Juhler NT, Korreman SS, Pedersen AN, Aarup LR, Nystrom H, Olsen M et al. Intra- and interfraction breathing variations during curative radiotherapy for lung cancer. Radiother Oncol 2007;84:40-8

4. Sonke JJ, Lebesque J, van Herk M. Variability of four-dimensional computed tomography patient models. Int J Radiat Oncol Biol Phys 2008;70:590-8
5. Sonke JJ, Rossi M, Wolthaus J, van Herk M, Damen E, Belderbos J. Frameless stereotactic body radiotherapy for lung cancer using four-dimensional cone beam CT guidance. Int J Radiat Oncol Biol Phys 2009;74:567-74
6. van Herk M, Witte M, Van der GJ, Schneider C, Lebesque JV. Biologic and physical fractionation effects of random geometric errors. Int J Radiat Oncol Biol Phys 2003;57:1460-71
7. International Commission on Radiation Units & Measurements. Prescribing, Recording, and Reporting Intensity-Modulated Photon-Beam Therapy (IMRT), ICRU Report 83. 2011.
8. International Commission on Radiation Units & Measurements (ICRU). Prescribing, Recording, and Reporting Photon Beam Therapy (Report 50). 1993.
9. International Commission on Radiation Units & Measurements (ICRU). Prescribing, Recording, and Reporting Photon Beam Therapy (Report 62), Supplement to ICRU Report 50. 1999.
10. Giraud P, Antoine M, Larrouy A, Milleron B, Callard P, De RY et al. Evaluation of microscopic tumor extension in non-small-cell lung cancer for three-dimensional conformal radiotherapy planning. Int J Radiat Oncol Biol Phys 2000;48:1015-24
11. Grills IS, Fitch DL, Goldstein NS, Yan D, Chmielewski GW, Welsh RJ et al. Clinicopathologic analysis of microscopic extension in lung adenocarcinoma: defining clinical target volume for radiotherapy. Int J Radiat Oncol Biol Phys 2007;69:334-41
12. Stroom J, Blaauwgeers H, van BA, Boersma L, Lebesque J, Theuws J et al. Feasibility of pathology-correlated lung imaging for accurate target definition of lung tumors. Int J Radiat Oncol Biol Phys 2007;69:267-75
13. McKenzie A, Coffey M, Crellin A, Dobbs J, Driver D, Greener T, Harrison A, Landberg T, Mijnheer B, Pitchford G, Sebag-Montefiore D, Smith K, Walker V. Geometric uncertainties in Radiotherapy: Defining the Planning Target Volume, The British Institute of Radiology. 2003. The British Institute of Radiology.
14. van Herk M. Errors and margins in radiotherapy. Semin Radiat Oncol 2004;14:52-64
15. van Herk M, Remeijer P, Rasch C, Lebesque JV. The probability of correct target dosage: dose-population histograms for deriving treatment margins in radiotherapy. Int J Radiat Oncol Biol Phys 2000;47:1121-35
16. McKenzie AL, van HM, Mijnheer B. The width of margins in radiotherapy treatment plans. Phys Med Biol 2000;45:3331-42
17. Killoran JH, Giraud JY, Chin L. A dosimetric comparison of two multileaf collimator designs. Med Phys 2002;29:1752-8
18. Mahesh M: MDCT Physics: The Basics - Technology, Image Quality and Radiation Dose. Lippincott Williams & Wilkins (Wolter Kluwer), 2009.
19. Chen GT, Kung JH, Beaudette KP. Artifacts in computed tomography scanning of moving objects. Semin Radiat Oncol 2004;14:19-26
20. Shimizu S, Shirato H, Kagei K, Nishioka T, Bo X, aka-Akita H et al. Impact of respiratory movement on the computed tomographic images of small lung tumors in three-dimensional (3D) radiotherapy. Int J Radiat Oncol Biol Phys 2000;46:1127-33
21. Rietzel E, Pan T, Chen GT. Four-dimensional computed tomography: image formation and clinical protocol. Med Phys 2005;32:874-89
22. Dinkel J, Welzel T, Bolte H, Hoffmann B, Thierfelder C, Mende U et al. Four-dimensional multislice helical CT of the lung: qualitative comparison of retrospectively gated and static images in an ex-vivo system. Radiother Oncol 2007;85:215-22
23. Yamamoto T, Langner U, Loo BW, Jr., Shen J, Keall PJ. Retrospective analysis of artifacts in four-dimensional CT images of 50 abdominal and thoracic radiotherapy patients. Int J Radiat Oncol Biol Phys 2008;72:1250-8
24. Liu HH, Balter P, Tutt T, Choi B, Zhang J, Wang C et al. Assessing respiration-induced tumor motion and internal target volume using four-dimensional computed tomography for radiotherapy of lung cancer. Int J Radiat Oncol Biol Phys 2007;68:531-40
25. Seppenwoolde Y, Shirato H, Kitamura K, Shimizu S, van HM, Lebesque JV et al. Precise and real-time measurement of 3D tumor motion in lung due to breathing and heartbeat, measured during radiotherapy. Int J Radiat Oncol Biol Phys 2002;53:822-34
26. Persson GF, Nygaard DE, Brink C, Jahn JW, Munck af RP, Specht L et al. Deviations in delineated GTV caused by artefacts in 4DCT. Radiother Oncol 2010;96:61-6
27. Shen S, Duan J, Fiveash JB, Brezovich IA, Plant BA, Spencer SA et al. Validation of target volume and position in respiratory gated CT planning and treatment. Med Phys 2003;30:3196-205
28. Pan T, Lee TY, Rietzel E, Chen GT. 4D-CT imaging of a volume influenced by respiratory motion on multi-slice CT. Med Phys 2004;31:333-40
29. Keall PJ, Starkschall G, Shukla H, Forster KM, Ortiz V, Stevens CW et al. Acquiring 4D thoracic CT scans using a multislice helical method. Phys Med Biol 2004;49:2053-67
30. Vedam SS, Keall PJ, Kini VR, Mostafavi H, Shukla HP, Mohan R. Acquiring a four-dimensional computed tomography dataset using an external respiratory signal. Phys Med Biol 2003;48:45-62
31. Low DA, Nystrom M, Kalinin E, Parikh P, Dempsey JF, Bradley JD et al. A method for the reconstruction of four-dimensional synchronized CT scans acquired during free breathing. Med Phys 2003;30:1254-63
32. Ford EC, Mageras GS, Yorke E, Ling CC. Respiration-correlated spiral CT: a method of measuring respiratory-induced anatomic motion for radiation treatment planning. Med Phys 2003;30:88-97
33. Li R, Lewis JH, Cervino LI, Jiang SB. 4D CT sorting based on patient internal anatomy. Phys Med Biol 2009;54:4821-33
34. Abdelnour AF, Nehmeh SA, Pan T, Humm JL, Vernon P, Schoder H et al. Phase and amplitude binning for 4D-CT imaging. Phys Med Biol 2007;52:3515-29
35. Lu W, Parikh PJ, Hubenschmidt JP, Bradley JD, Low DA. A comparison between amplitude sorting and phase-angle sorting using external respiratory measurement for 4D CT. Med Phys 2006;33:2964-74
36. Olsen JR, Lu W, Hubenschmidt JP, Nystrom MM, Klahr P, Bradley JD et al. Effect of novel amplitude/phase binning algorithm on commercial four-dimensional computed tomography quality. Int J Radiat Oncol Biol Phys 2008;70:243-52
37. Vorwerk H, Beckmann G, Bremer M, Degen M, Dietl B, Fietkau R et al. The delineation of target volumes for radiotherapy of lung cancer patients. Radiother Oncol 2009;91:455-60

38. Steenbakkers RJ, Duppen JC, Fitton I, Deurloo KE, Zijp LJ, Comans EF et al. Reduction of observer variation using matched CT-PET for lung cancer delineation: a three-dimensional analysis. Int J Radiat Oncol Biol Phys 2006;64:435-48
39. Kepka L, Bujko K, Garmol D, Palucki J, Zolciak-Siwinska A, Guzel-Szczepiorkowska Z et al. Delineation variation of lymph node stations for treatment planning in lung cancer radiotherapy. Radiother Oncol 2007;85:450-5
40. Giraud P, Elles S, Helfre S, De RY, Servois V, Carette MF et al. Conformal radiotherapy for lung cancer: different delineation of the gross tumor volume (GTV) by radiologists and radiation oncologists. Radiother Oncol 2002;62:27-36
41. Fitzpatrick MJ, Starkschall G, Antolak JA, Fu J, Shukla H, Keall PJ et al. Displacement-based binning of time-dependent computed tomography image data sets. Med Phys 2006;33:235-46
42. Ashamalla H, Rafla S, Parikh K, Mokhtar B, Goswami G, Kambam S et al. The contribution of integrated PET/CT to the evolving definition of treatment volumes in radiation treatment planning in lung cancer. Int J Radiat Oncol Biol Phys 2005;63:1016-23
43. Hanna GG, McAleese J, Carson KJ, Stewart DP, Cosgrove VP, Eakin RL et al. (18)F-FDG PET-CT simulation for non-small-cell lung cancer: effect in patients already staged by PET-CT. Int J Radiat Oncol Biol Phys 2010;77:24-30
44. Faria SL, Menard S, Devic S, Sirois C, Souhami L, Lisbona R et al. Impact of FDG-PET/CT on radiotherapy volume delineation in non-small-cell lung cancer and correlation of imaging stage with pathologic findings. Int J Radiat Oncol Biol Phys 2008;70:1035-8
45. Spratt DE, Diaz R, McElmurray J, Csiki I, Duggan D, Lu B et al. Impact of FDG PET/CT on delineation of the gross tumor volume for radiation planning in non-small-cell lung cancer. Clin Nucl Med 2010;35:237-43
46. Bradley J, Thorstad WL, Mutic S, Miller TR, Dehdashti F, Siegel BA et al. Impact of FDG-PET on radiation therapy volume delineation in non-small-cell lung cancer. Int J Radiat Oncol Biol Phys 2004;59:78-86
47. Fitton I, Steenbakkers RJ, Gilhuijs K, Duppen JC, Nowak PJ, van HM et al. Impact of anatomical location on value of CT-PET co-registration for delineation of lung tumors. Int J Radiat Oncol Biol Phys 2008;70:1403-7
48. Roy AE, Wells P. Volume definition in radiotherapy planning for lung cancer: how the radiologist can help. Cancer Imaging 2006;6:116-23
49. De RD, Faivre-Finn C, Nestle U, Hurkmans CW, Le PC, Price A et al. European organisation for research and treatment of cancer recommendations for planning and delivery of high-dose, high-precision radiotherapy for lung cancer. J Clin Oncol 2010;28:5301-10
50. Kini VR, Vedam SS, Keall PJ, Patil S, Chen C, Mohan R. Patient training in respiratory-gated radiotherapy. Med Dosim 2003;28:7-11
51. George R, Chung TD, Vedam SS, Ramakrishnan V, Mohan R, Weiss E et al. Audio-visual biofeedback for respiratory-gated radiotherapy: impact of audio instruction and audio-visual biofeedback on respiratory-gated radiotherapy. Int J Radiat Oncol Biol Phys 2006;65:924-33
52. Keall PJ, Mageras GS, Balter JM, Emery RS, Forster KM, Jiang SB et al. The management of respiratory motion in radiation oncology report of AAPM Task Group 76. Med Phys 2006;33:3874-900
53. Wolthaus JW, Schneider C, Sonke JJ, van HM, Belderbos JS, Rossi MM et al. Mid-ventilation CT scan construction from four-dimensional respiration-correlated CT scans for radiotherapy planning of lung cancer patients. Int J Radiat Oncol Biol Phys 2006;65:1560-71
54. Underberg RW, Lagerwaard FJ, Cuijpers JP, Slotman BJ, van Sornsen de Koste JR, Senan S. Four-dimensional CT scans for treatment planning in stereotactic radiotherapy for stage I lung cancer. Int J Radiat Oncol Biol Phys 2004;60:1283-90
55. Underberg RW, Lagerwaard FJ, Slotman BJ, Cuijpers JP, Senan S. Use of maximum intensity projections (MIP) for target volume generation in 4DCT scans for lung cancer. Int J Radiat Oncol Biol Phys 2005;63:253-60
56. Wolthaus JW, Sonke JJ, van HM, Belderbos JS, Rossi MM, Lebesque JV et al. Comparison of different strategies to use four-dimensional computed tomography in treatment planning for lung cancer patients. Int J Radiat Oncol Biol Phys 2008;70:1229-38
57. Keall P, Vedam S, George R, Bartee C, Siebers J, Lerma F et al. The clinical implementation of respiratory-gated intensity-modulated radiotherapy. Med Dosim 2006;31:152-62
58. Berson AM, Emery R, Rodriguez L, Richards GM, Ng T, Sanghavi S et al. Clinical experience using respiratory gated radiation therapy: comparison of free-breathing and breath-hold techniques. Int J Radiat Oncol Biol Phys 2004;60:419-26
59. McNair HA, Brock J, Symonds-Tayler JR, Ashley S, Eagle S, Evans PM et al. Feasibility of the use of the Active Breathing Co ordinator (ABC) in patients receiving radical radiotherapy for non-small cell lung cancer (NSCLC). Radiother Oncol 2009;93:424-9
60. Brock J, McNair HA, Panakis N, Symonds-Tayler R, Evans PM, Brada M. The Use of the Active Breathing Coordinator throughout Radical Non-small-cell Lung Cancer (NSCLC) Radiotherapy. Int J Radiat Oncol Biol Phys 2010;
61. Sonke JJ, Zijp L, Remeijer P, van HM. Respiratory correlated cone beam CT. Med Phys 2005;32:1176-86
62. Purdie TG, Moseley DJ, Bissonnette JP, Sharpe MB, Franks K, Bezjak A et al. Respiration correlated cone-beam computed tomography and 4DCT for evaluating target motion in Stereotactic Lung Radiation Therapy. Acta Oncol 2006;45:915-22
63. Li T, Xing L, Munro P, McGuinness C, Chao M, Yang Y et al. Four-dimensional cone-beam computed tomography using an on-board imager. Med Phys 2006;33:3825-33
64. Gottlieb KL, Hansen CR, Hansen O, Westberg J, Brink C. Investigation of respiration induced intra- and inter-fractional tumour motion using a standard Cone Beam CT. Acta Oncol 2010;49:1192-8
65. Ottosson W, Baker M, Hedman M, Behrens CF, Sjostrom D. Evaluation of setup accuracy for NSCLC patients; studying the impact of different types of cone-beam CT matches based on whole thorax, columna vertebralis, and GTV. Acta Oncol 2010;49:1184-91
66. Purdie TG, Bissonnette JP, Franks K, Bezjak A, Payne D, Sie F et al. Cone-beam computed tomography for on-line image guidance of lung stereotactic radiotherapy: localization, verification, and intrafraction tumor position. Int J Radiat Oncol Biol Phys 2007;68:243-52
67. Grills IS, Hugo G, Kestin LL, Galerani AP, Chao KK, Wloch J et al. Image-guided radiotherapy via daily online cone-beam CT substantially reduces margin requirements for stereotactic lung radiotherapy. Int J Radiat Oncol Biol Phys 2008;70:1045-56

68. Korreman SS, Persson GF, Nygaard DE, Brink C. Lung Cancer Radiotherapy with Respiratory Management: The Effect of Beam Gating on Treatment Field Margins is Negligible. International Journal of Radiation Oncology*Biology*Physics 2009;75:S75
69. Guckenberger M, Krieger T, Richter A, Baier K, Wilbert J, Sweeney RA, Flentje M. Potential of image-guidance, gating and real-time tracking to improve accuracy in pulmonary stereotactic body radiotherapy. Radiotherapy and Oncology 91[3], 288-295. 1-6-2009
70. Sonke JJ, Zijp L, Remeijer P, van Herk M. Respiratory correlated cone beam CT. Med Phys 2005;32:1176-86
71. Hanley J, Debois MM, Mah D, Mageras GS, Raben A, Rosenzweig K et al. Deep inspiration breath-hold technique for lung tumors: the potential value of target immobilization and reduced lung density in dose escalation. Int J Radiat Oncol Biol Phys 1999;45:603-11
72. Guckenberger M, Kavanagh A, Webb S, Brada M. A novel respiratory motion compensation strategy combining gated beam delivery and mean target position concept - A compromise between small safety margins and long duty cycles. Radiother Oncol 2011;98:317-22
73. van der Voort van Zyp NC, Prevost JB, Hoogeman MS, Praag J, van der HB, Levendag PC et al. Stereotactic radiotherapy with real-time tumor tracking for non-small cell lung cancer: clinical outcome. Radiother Oncol 2009;91:296-300
74. Whyte RI, Crownover R, Murphy MJ, Martin DP, Rice TW, DeCamp MM, Jr. et al. Stereotactic radiosurgery for lung tumors: preliminary report of a phase I trial. Ann Thorac Surg 2003;75:1097-101
75. Wilbert J, Meyer J, Baier K, Guckenberger M, Herrmann C, Hess R et al. Tumor tracking and motion compensation with an adaptive tumor tracking system (ATTS): system description and prototype testing. Med Phys 2008;35:3911-21
76. Falk M, af Rosenschold PM, Keall P, Cattell H, Cho BC, Poulsen P et al. Real-time dynamic MLC tracking for inversely optimized arc radiotherapy. Radiother Oncol 2010;94:218-23
77. Zimmermann FB, Geinitz H, Schill S, Thamm R, Nieder C, Schratzenstaller U et al. Stereotactic hypofractionated radiotherapy in stage I (T1-2 N0 M0) non-small-cell lung cancer (NSCLC). Acta Oncol 2006;45:796-801
78. Neicu T, Shirato H, Seppenwoolde Y, Jiang SB. Synchronized moving aperture radiation therapy (SMART): average tumour trajectory for lung patients. Phys Med Biol 2003;48:587-98
79. Keall PJ, Cattell H, Pokhrel D, Dieterich S, Wong KH, Murphy MJ et al. Geometric accuracy of a real-time target tracking system with dynamic multileaf collimator tracking system. International Journal of Radiation Oncology*Biology*Physics 2006;65:1579-84
80. Benedict SH, Yenice KM, Followill D, Galvin JM, Hinson W, Kavanagh B et al. Stereotactic body radiation therapy: the report of AAPM Task Group 101. Med Phys 2010;37:4078-101
81. Lax I, Blomgren H, Naslund I, Svanstrom R. Stereotactic radiotherapy of malignancies in the abdomen. Methodological aspects. Acta Oncol 1994;33:677-83
82. Masashi K, Yoshihiro T, Yoshihiro O, Haruo M, Ken T, Chiaki T et al. A phase II study on stereotactic body radiotherapy for stage I non-small cell lung cancer. Radiother Oncol 2007;85:429-34
83. Umberto R, Andrea RF, Alessia G, Francesca RG, Patrizia C, Pierfrancesco F, Cristina M, Piero B, Giorgio VS, Riccardo R. Stereotactic body radiation therapy for early stage non-small cell lung cancer: Results of a prospective trial. Lung cancer (Amsterdam, Netherlands) 68[1], 72-77. 1-4-2010
84. Baumann P, Nyman J, Hoyer M, Wennberg B, Gagliardi G, Lax I et al. Outcome in a Prospective Phase II Trial of Medically Inoperable Stage I Non Small-Cell Lung Cancer Patients Treated With Stereotactic Body Radiotherapy. Journal of Clinical Oncology 2009;27:3290-6
85. Timmerman R, Paulus R, Galvin J, Michalski J, Straube W, Bradley J et al. Stereotactic Body Radiation Therapy for Inoperable Early Stage Lung Cancer. JAMA: The Journal of the American Medical Association 2010;303:1070-6
86. Achilles JF, Ronald CM, Constantin TY, Lech P, Mark W, Mark AH et al. Stereotactic Body Radiation Therapy for Early-Stage Non Small-Cell Lung Carcinoma: Four-Year Results of a Prospective Phase II Study. Int J Radiat Oncol Biol Phys 2009;75:677-82
87. Guckenberger M, Wilbert J, Krieger T, Richter A, Baier K, Meyer J et al. Four-Dimensional Treatment Planning for Stereotactic Body Radiotherapy. International Journal of Radiation Oncology*Biology*Physics 2007;69:276-85
88. Onimaru R, Fujino M, Yamazaki K, Onodera Y, Taguchi H, Katoh N et al. Steep Dose-Response Relationship for Stage I Non-Small-Cell Lung Cancer using Hypofractionated High-Dose Irradiation by Real-Time Tumor-Tracking Radiotherapy. Int J Radiat Oncol Biol Phys 2007;
89. Wulf J, Baier K, Mueller G, Flentje MP. Dose-response in stereotactic irradiation of lung tumors. Radiotherapy and Oncology 2005;77:83-7
90. Jensen HR, Hansen O, Hjelm-Hansen M, Brink C. Inter- and intrafractional movement of the tumour in extracranial stereotactic radiotherapy of NSCLC. Acta Oncol 2008;47:1432-7
91. VassarStats; Web Site for Statistical Computation [Homepage on the Internet]. Vassar College, Poughkeepsie, NY, US. [Accessed 11-10-2010] Available from http://faculty.vassar.edu/lowry/VassarStats.html
92. Senan S, van Sornsen de KJ, Samson M, Tankink H, Jansen P, Nowak PJ et al. Evaluation of a target contouring protocol for 3D conformal radiotherapy in non-small cell lung cancer. Radiother Oncol 1999;53:247-55
93. Van de Steene J, Linthout N, de Mey J, Vinh-Hung V, Claassens C, Noppen M et al. Definition of gross tumor volume in lung cancer: inter-observer variability. Radiother Oncol 2002;62:37-49
94. van LJ, Siedschlag C, Stroom J, Blauwgeers H, van Suylen RJ, Knegjens J et al. Microscopic Disease Extension in Three Dimensions for Non-Small-Cell Lung Cancer: Development of a Prediction Model Using Pathology-Validated Positron Emission Tomography and Computed Tomography Features. Int J Radiat Oncol Biol Phys 2010;
95. Siedschlag C, van LJ, van BA, Rossi MM, van PR, Blaauwgeers JL et al. Analysis of the relative deformation of lung lobes before and after surgery in patients with NSCLC. Phys Med Biol 2009;54:5483-92
96. Hanna GG, Hounsell AR, O'Sullivan JM. Geometrical analysis of radiotherapy target volume delineation: a systematic review of reported comparison methods. Clin Oncol (R Coll Radiol) 2010;22:515-25
97. Persson GF, Nygaard DE, Munck af Rosenschold P., Vogelius IR, Josipovic M, Specht L et al. Artifacts in conventional computed tomography (CT) and free breathing four-dimensional CT induce uncertainty in gross tumor volume determination. Int J Radiat Oncol Biol Phys 2010;

98. Nakamura M, Narita Y, Sawada A, Matsugi K, Nakata M, Matsuo Y et al. Impact of motion velocity on four-dimensional target volumes: a phantom study. Med Phys 2009;36:1610-7
99. Sarker J, Chu A, Mui K, Wolfgang JA, Hirsch AE, Chen GT et al. Variations in tumor size and position due to irregular breathing in 4D-CT: a simulation study. Med Phys 2010;37:1254-60
100. Watkins WT, Li R, Lewis J, Park JC, Sandhu A, Jiang SB et al. Patient-specific motion artifacts in 4DCT. Medical Physics 2010;37:2855-61
101. Korreman SS, Ulrich S, Bowen S, Deveau M, Bentzen SM, Jeraj R. Feasibility of dose painting using volumetric modulated arc optimization and delivery. Acta Oncol 2010;49:964-71
102. Guckenberger M, Weininger M, Wilbert J, Richter A, Baier K, Krieger T et al. Influence of retrospective sorting on image quality in respiratory correlated computed tomography. Radiother Oncol 2007;85:223-31
103. Langner UW, Keall PJ. Accuracy in the localization of thoracic and abdominal tumors using respiratory displacement, velocity, and phase. Med Phys 2009;36:386-93
104. Langner UW, Keall PJ. Prospective displacement and velocity-based cine 4D CT. Med Phys 2008;35:4501-12
105. Langner UW, Keall PJ. Quantification of artifact reduction with real-time cine four-dimensional computed tomography acquisition methods. Int J Radiat Oncol Biol Phys 2010;76:1242-50
106. Korreman S, Mostafavi H, Le QT, Boyer A. Comparison of respiratory surrogates for gated lung radiotherapy without internal fiducials. Acta Oncol 2006;45:935-42
107. Vedam SS, Kini VR, Keall PJ, Ramakrishnan V, Mostafavi H, Mohan R. Quantifying the predictability of diaphragm motion during respiration with a noninvasive external marker. Med Phys 2003;30:505-13
108. George R, Ramakrishnan V, Siebers JV, Chung TD, Keall PJ. Investigation of patient, tumour and treatment variables affecting residual motion for respiratory-gated radiotherapy. Phys Med Biol 2006;51:5305-19
109. Neicu T, Berbeco R, Wolfgang J, Jiang SB. Synchronized moving aperture radiation therapy (SMART): improvement of breathing pattern reproducibility using respiratory coaching. Phys Med Biol 2006;51:617-36
110. Venkat RB, Sawant A, Suh Y, George R, Keall PJ. Development and preliminary evaluation of a prototype audiovisual biofeedback device incorporating a patient-specific guiding waveform. Phys Med Biol 2008;53:N197-N208
111. Cui G, Gopalan S, Yamamoto T, Berger J, Maxim PG, Keall PJ. Commissioning and quality assurance for a respiratory training system based on audiovisual biofeedback. J Appl Clin Med Phys 2010;11:3262
112. Haasbeek CJ, Spoelstra FO, Lagerwaard FJ, van Sornsen de Koste JR, Cuijpers JP, Slotman BJ et al. Impact of audio-coaching on the position of lung tumors. Int J Radiat Oncol Biol Phys 2008;71:1118-23
113. Court L, Wagar M, Berbeco R, Reisner A, Winey B, Schofield D et al. Evaluation of the interplay effect when using RapidArc to treat targets moving in the craniocaudal or right-left direction. Med Phys 2010;37:4-11
114. Guckenberger M, Meyer J, Wilbert J, Richter A, Baier K, Mueller G et al. Intra-fractional uncertainties in cone-beam CT based image-guided radiotherapy (IGRT) of pulmonary tumors. Radiother Oncol 2007.